Sistemas Hidrotermais e Metalogênese

GSA 0407

MINERALIZAÇÕES EPITERMAIS

Caetano Juliani
(cjuliani@usp.br)
Lena Virgínia Soares Monteiro
(lena.monteiro@usp.br)

Departamento de Geologia Sedimentar e Ambiental
2019

FAA - NEXT GENERATION EXPLORERS AWARD

Em nome da *Next Generation Explorers Award Association*, temos o prazer de anunciar que as inscrições para o Prêmio Frank Arnott estão abertas.

O Prêmio Frank Arnott é uma competição internacional em que equipes de estudantes universitários de geociências, com ênfase na mineração, colaboram e inovam para transformar os conjuntos de dados de geociências em sua interpretação dos alvos subterrâneos de geologia e mineralização.

As equipes finalistas apresentarão seus resultados para um painel ao vivo de juízes e público, durante o PDAC de 2021. Esta é uma ótima oportunidade para obter experiências do "mundo real" com conjuntos de dados modernos, além de reconhecimento internacional.

Como estudantes, vemos que a participação nesta competição aumentará sua rede com a indústria, além de oportunidades de emprego. Para as universidades, a competição pode aumentar o seu reconhecimento como uma universidade líder na comunidade de geociências com ênfase em mineração e aumentar o potencial de atrair futuros alunos e financiamento adicional.

Para inscrever sua equipe ou saber mais sobre o Prêmio Frank Arnott, acesse www.frankarnottaward.com ou envie um e-mail para
info@NextGenerationExplorersAward@gmail.com

Sinceramente,
Next Generation Explorers Award Committee

FAA - NEXT GENERATION EXPLORERS AWARD

Background | Concept | About Frank | How to Enter | Datasets | Sponsorship | Contact

Background

Frank Arnott - Next Generation Explorers Award is a follow up to the Frank Arnott Award (FAA) 2017, founded in honour of Frank Arnott (1951-2009); an exceptional exploration industry leader who championed innovative techniques that maximized the value of the multidisciplinary data underpinning exploration campaigns worldwide.

Recognizing that effective data integration and visualization of data remains one of the biggest challenges, the Frank Arnott Award 'collaborative' challenge, focused on innovation in data integration and visualization, was launched in 2016. Participants selected one of five high quality global datasets and submissions were entered from around the globe in April of 2017. Evaluated by independent judges, the top 3 teams in both the Experienced and Apprentice categories were selected and honoured during the prestigious Exploration 2017 Decennial Mining Exploration Conference (DMEC). Each finalist team gave a presentation of their project findings and were formally presented with their final ranking and award October 24th 2017 in Toronto, Canada.

Given the success of the Frank Arnott Award and the opportunity that it presented for students worldwide, with the combined efforts of various sponsors and endorsements the challenge will continue.

Gold Deposits

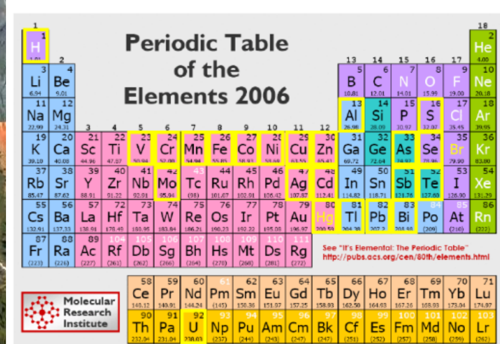

High Sulfidation Epithermal Gold Deposits

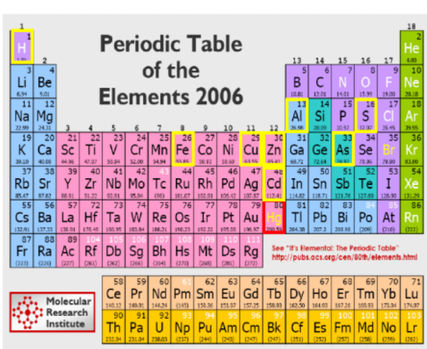

J.P. Richards / Ore Geology Reviews 40 (2011) 1–26 13

Epitermais

Pórfiros

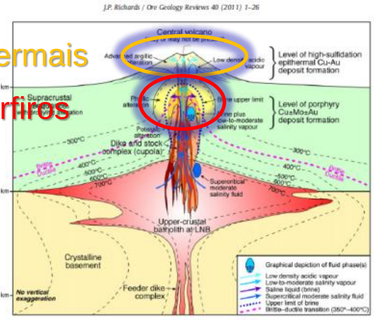

Fig. 7. Schematic cross-section through a typical coupled arc batholith–cupola–volcanic system, with associated porphyry Cu ± Au and linked high sulfidation Cu–Au epithermal deposits. Also shown are the thermal structure, fluid flow pathways and characteristics during the main stage of hydrothermal activity, and overlapping hydrothermal alteration zones. Propylitic alteration by circulating heated groundwaters can be assumed to affect all the supracrustal rocks in the field of view, with greatest intensity (epidote, actinolite) close to the intrusions, fading to background distally. Modified from Richards (2005); sources: Sillitoe (1973, 2010), Dilles (1987), Shinohara and Hedenquist (1997), Hedenquist et al. (1998), and Fournier (1999).

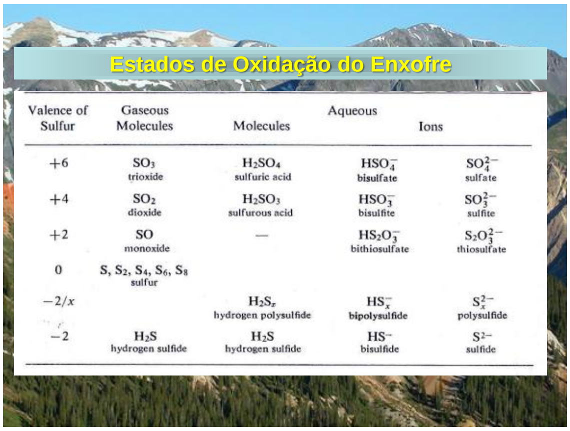

Valence of Sulfur	Gaseous Molecules	Aqueous Molecules	Aqueous Ions	
+6	SO_3 trioxide	H_2SO_4 sulfuric acid	HSO_4^- bisulfate	SO_4^{2-} sulfate
+4	SO_2 dioxide	H_2SO_3 sulfurous acid	HSO_3^- bisulfite	SO_3^{2-} sulfite
+2	SO monoxide	—	$HS_2O_3^-$ bithiosulfate	$S_2O_3^{2-}$ thiosulfate
0	S, S_2, S_4, S_6, S_8 sulfur			
$-2/x$		H_2S_x hydrogen polysulfide	HS_x^- bipolysulfide	S_x^{2-} polysulfide
−2	H_2S hydrogen sulfide	H_2S hydrogen sulfide	HS^- bisulfide	S^{2-} sulfide

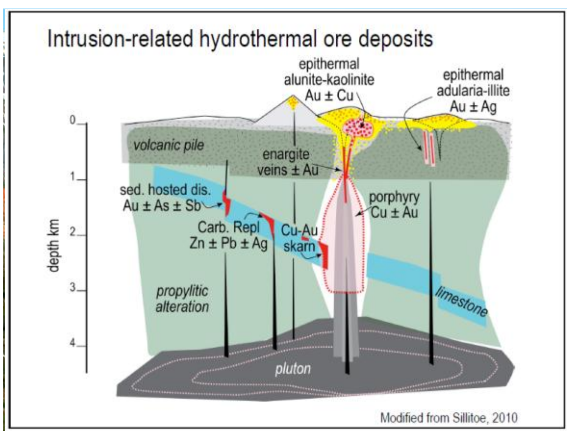

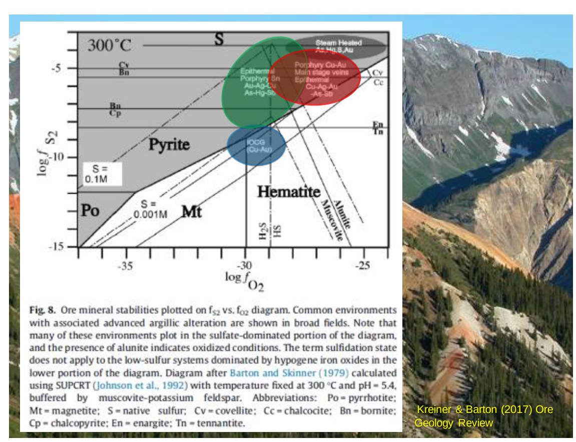

Fig. 8. Ore mineral stabilities plotted on f_{S2} vs. f_{O2} diagram. Common environments with associated advanced argillic alteration are shown in broad fields. Note that many of these environments plot in the sulfate-dominated portion of the diagram, and the presence of alunite indicates oxidized conditions. The term sulfidation state does not apply to the low-sulfur systems dominated by hypogene iron oxides in the lower portion of the diagram. Diagram after Barton and Skinner (1979) calculated using SUPCRT (Johnson et al., 1992) with temperature fixed at 300 °C and pH = 5.4, buffered by muscovite-potassium feldspar. Abbreviations: Po = pyrrhotite; Mt = magnetite; S = native sulfur; Cv = covellite; Cc = chalcocite; Bn = bornite; Cp = chalcopyrite; En = enargite; Tn = tennantite.

Kreiner & Barton (2017) Ore Geology Review

Mineralizações epitermais

1) Forma-se em temperaturas entre 200 e 300 ºC, com variações para < 150 a >400 ºC)

2) Formam-se em profundidades rasas ou superficiais (pressões baixas), alcançando até ~ 2 km (normalmente formam-se a poucas centenas de metros de profundidade)

3) Associam-se predominantemente a vulcanismo intermediário e félsico e arcos magmáticos continentais e insulares, sistemas oceânicos - principalmente em bacias de *back-arc* e em magmatismo intraplaca

4) Se relacionam com caldeiras vulcânicas

► Deposição do conteúdo metalífero dos fluídos nas zonas de *boiling*, indicando que os corpos mineralizados não tem continuidade em profundidade nas falhas

► A concentração dos corpos mineralizados estão numa zona de pouco mais de 300 metros de espessura

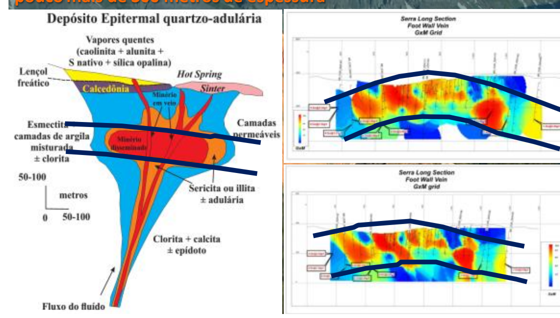

CARACTERÍSTICAS GEOLÓGICAS GERAIS DA MINERALIÇÕE EPITERMAIS

- *Rochas hospedeiras*: vulcânicas de composição cálcio-alcalina ou alcalina ➔ andesitos, dacitos, riodacitos, riolitos (raramente basaltos) e ➔ vulcanoclásticas piroclásticas a epiclásticas ➔ rochas (meta)sedimentares ➔ rochas do embasamento das vulcânicas

- Mineralização em sistemas de fraturas e/ou falhas ➔ estruturas extensionais, às vezes associadas a estruturas de colapso em zonas de caldeira, brechas hidrotermais ➔ circulação mais efetiva de fluidos.

- Mineralização em veios (1-10 m de espessura) de alto ângulo, sistema de veios ou *stockworks* e disseminada. Mineralização extensa ao longo da direção, mas restrita em profundidade (500 a 1500 m, média de 350 m).

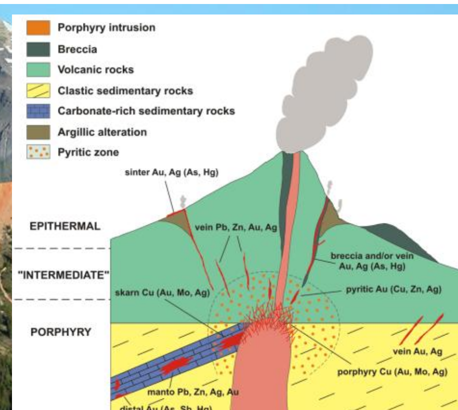

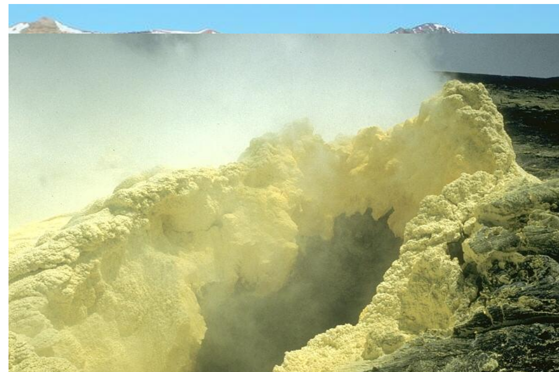

Fumarola no Kilauewa

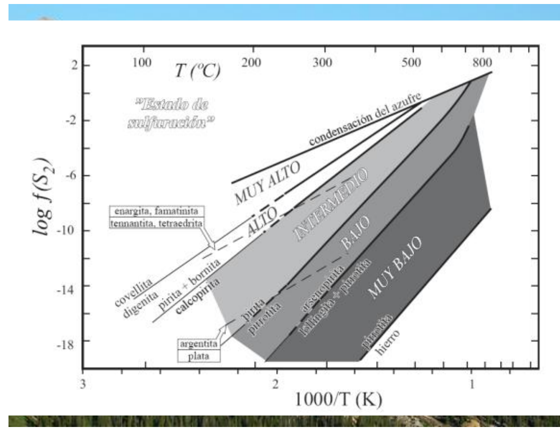

Goldfield type	Hedenquist (2005), baseado em Sillitoe & Hedenquist (2003) e Einaudi *et al.* (2003)		Ransome (1907)
Alunitic kaolinic gold veins	Sericitic zinc-silver veins	Gold-silver-adularia veins Fluoritic tellurium-adularia gold veins	Emmons (1918)
Gold-alunite deposits	Gold-quartz veins in andesite		Lindgren (1933)
	Argentite-gold quartz veins Argentite veins Base metal veins	Gold-quartz veins in rhyolite Gold telluride veins Gold selenide veins	
Secondary quartzite (Altered host rock)			Fedorov (1903); Nakovnik (1933)
Acid	Alkaline		Sillitoe (1977)
Epithermal			Buchanan (1981)
Enargite-gold			Ashley (1982)
		Hot-spring type	Giles and Nelson (1982)
High sulfur	Low sulfur		Bonham (1986, 1988)
Acid sulfate	Adularia-sericite		Hayba et al. (1985), Heald et al. (1987)
High sulfidation	Low sulfidation		Hedenquist (1987)
Alunite-kaolinite	Adularia-sericite		Berger and Henley (1989)
	Type 1 adularia-sericite	Type 2 adularia-sericite	Albino and Margolis (1991)
High sulfidation	High sulfide + base metal, low sulfidation	Low sulfide + base metal, low sulfidation	Sillitoe (1993)
Lithocap (Altered host rock)			Sillitoe (1995)
High sulfidation	Western andesite assemblage, low sulfidation	Bimodal basalt-rhyolite assemblage, low sulfidation	John et al. (1999); John (2001)
High sulfidation (HS)	Intermediate sulfidation (IS)	Low sulfidation (LS)	Hedenquist et al. (2000)

OS DOIS SUB-TIPOS PRINCIPAIS:

Associação mineral diagnóstica: ***High-Sulfidation (HS)***
Quartzo + Alunita ± Pirofilita ± Dickita ± Caolinita

Indica: pH ácido e condições oxidantes (H_2SO_4)
↖ Sulfato

Associação mineral diagnóstica: ***Low-Sulfidation (LS)***
Quartzo ± Calcita ± Adulária ± Illita (Sericita)

Indica: pH ~ neutro (ao redor de 7) a levemente alcalino e condições redutoras (H_2S)
↖ Sulfeto

Segundo as classificações de Hedenquist (1987) e White & Hedenquist (1990, 1995)

CONDIÇÕES REDOX E pH DOS FLUIDOS MINERALIZANTES

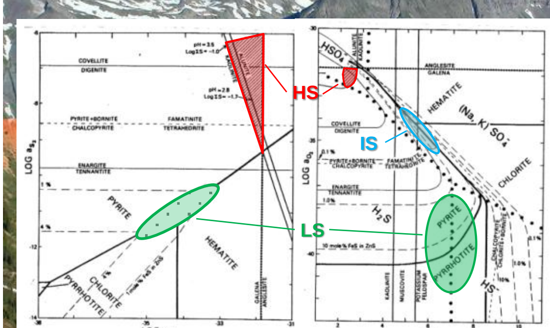

UM TERCEIRO SUB-TIPO IMPORTANTE:

Associação mineral diagnóstica:
Quartzo + Illita/Sericita + Sulfetos de metais de base relativament abundantes (calcopirita, esfalerita, galena) + Carbonatos (Calcita manganesífera e/or rodocrosita) ± Piemontita
(Alunita, Pirofilita e Adulária ausentes ou ocasionais)

Indica: pH ~ neutro e condições levemente oxidantes
↖ Sulfetos

Intermediate-Sulfidation (IS) ou Base Metals Epithermal

Segundo as classificações de Hedenquist (1987) e White & Hedenquist (1990, 1995)

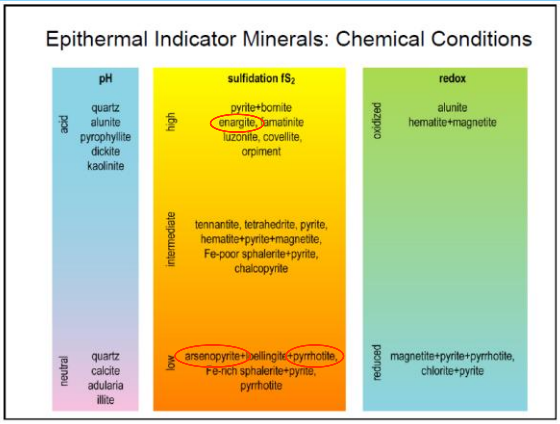

	VERY LOW	LOW	INTERMEDIATE		HIGH		VERY HIGH
	löl+po+S_2=asp	löl+S_2=asp+As	po+S_2=py mgt+S_2=hem+py		ten+S_2=enar cpy+py+S_2=bor		dig+S_2=cov
SYSTEM	1	2	3	4	5	6	7
Fe-S	pyrrhotite <p>(po)	pyrrhotite	pyrrhotite	pyrite (py)	pyrite	pyrite	pyrite, S
As-S	As	As	As	As	*realgar, orpiment*	*orpiment*, AsS glass	AsS glass
Fe-As-S	*löllingite+po, löllingite*	*löllingite*, arsenopyrite (asp)	arsenopyrite	Arsenopyrit *py+asp, py+As*			
Cu-S	chalcocite	chalcocite	chalcocite, digenite	digenite	digenite	digenite	*covellite*
Cu-Fe-S	chalcopyrite (cpy) + pyrrhotite	chalcopyrite (cpy) + pyrrhotite	Chalcopyrite +pyrrhotite	*chalcopy + pyrite*	*Chalcopy +pyrite*	*bornite bor)+py, digenite +pyrite*	*digenite +pyrite*
Cu-Fe-As-S	*löl+bor, löl + cpy*	*asp+cpy, löl+cpy*, asp+tennan	*asp+cpy*, asp + tennantite	asp+tennan, *asp+py*	enargite	enargite	enargite
Cu-Fe-S-O	magnetite (mgt)+ bornite, mgt+cpy	mgt+bor, mgt+cpy	mgt+bor, mgt+cpy	mgt+bor, mgt+cpy, *mgt+py*	mgt+cpy, hematite (hm) +py	hem+py	hem+py
OTHER	Bi, Ag, Hg, Sb, *Sb+po,* galena(gal)+hematite	Bi, Ag, Hg, Sb, *Sb+po*, galena(gal) +hematite	Bi, Ag, Hg, Sb, bismuthinit, stibnite, gal+ hem, argentite, berthierite	Bismuthinit (bis), argentite, berthierite, cinnabar, stibnite(stb), gal+hem, stb+py	bis, arg, cin, stb, gal+hem, anglesite +py, stb+py, famatinite	bis, arg, cin, stb, stb+py, anglesite +py, famatinite	bis, arg, cin, stb, stb+py, anglsite+py, famatinite
mol%FeS in Sphalerite Coexisting with Fe-sulf	>40	40-35	35-20	20-5	5-0.1	0.1-0.01	<0.01

Enargita, Cu_3AsS_4, ortorrômbica, preto acinzentado a preto, metálico, dureza 3.
Luzonita: Tetragonal, dureza 3,5

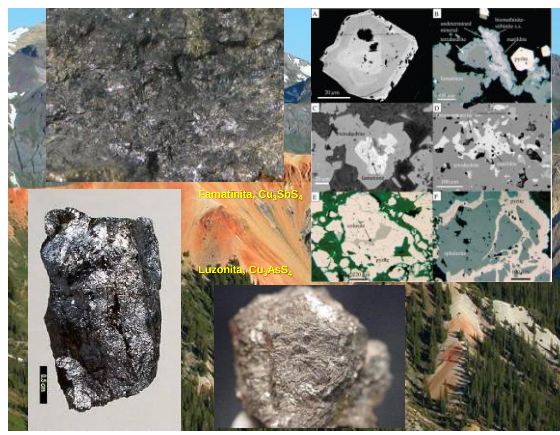

Covellita (CuS), dureza:,5-2, hexagonal

Svanbergite: $SrAl_3(PO_4)(SO_4)(OH)_6$

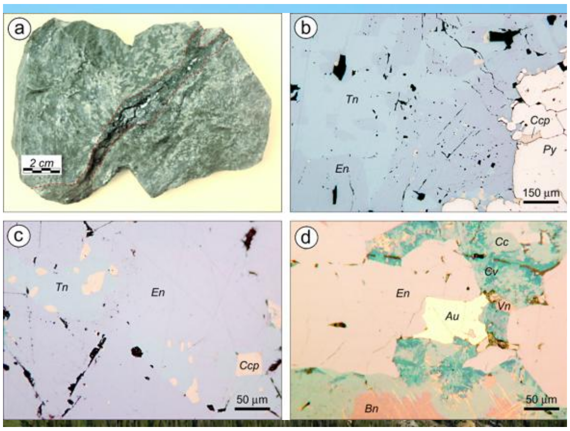
a
2 cm
b
Tn
Ccp
Py
En
150 µm
c
Tn
En
Ccp
50 µm
d
Cc
Cv
En
Au
Vn
Bn
50 µm


Lollingita (FeAs2), ortorrômbico, cinza-aço a prateado, metálico, dureza 5,0 a 5,5


Alunita
KAl3(SO4)2(OH)6
Trigonal
Dureza: 3,5 – 4,0
Cor: amarela, vermelha, marrom-avermelhado, branca, rósea, cinza, incolor

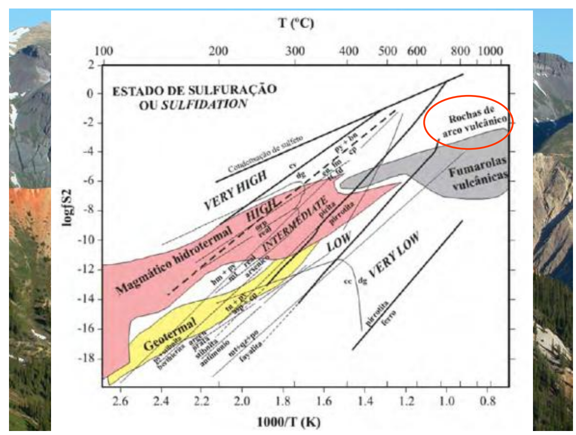
T (°C)
100
200
300
400
500
600
800
1000
ESTADO DE SULFURAÇÃO
OU SULFIDATION
Rochas de arco vulcânico
Fumarolas vulcânicas
VERY HIGH
HIGH
INTERMEDIATE
LOW
VERY LOW
Magmático hidrotermal
Geotermal
logfS2
1000/T (K)

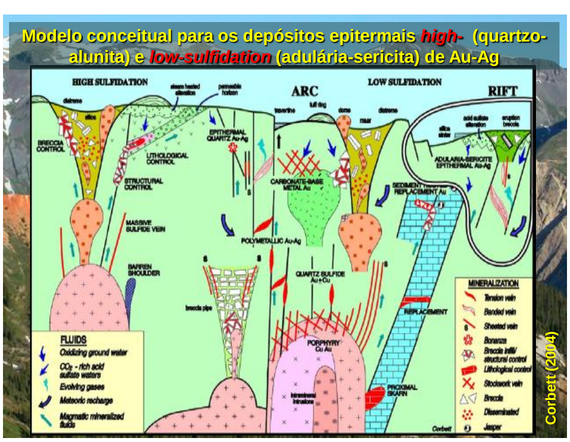
Modelo conceitual para os depósitos epitermais high- (quartzo-alunita) e low-sulfidation (adulária-sericita) de Au-Ag
HIGH SULFIDATION
ARC
LOW SULFIDATION
RIFT
FLUIDS
MINERALIZATION
Corbett (2004)

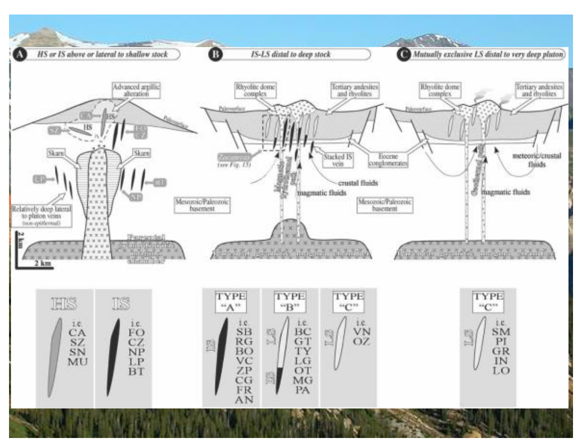
HIS
IS
TYPE "A"
TYPE "B"
TYPE "C"
TYPE "C"

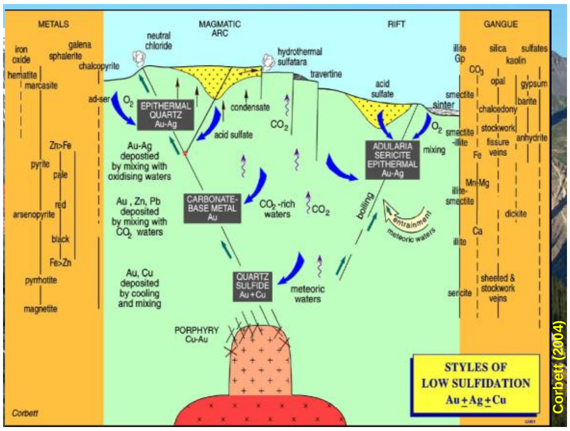

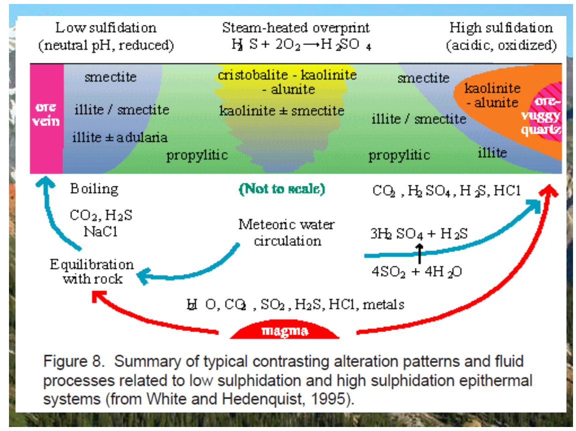

Figure 8. Summary of typical contrasting alteration patterns and fluid processes related to low sulphidation and high sulphidation epithermal systems (from White and Hedenquist, 1995).

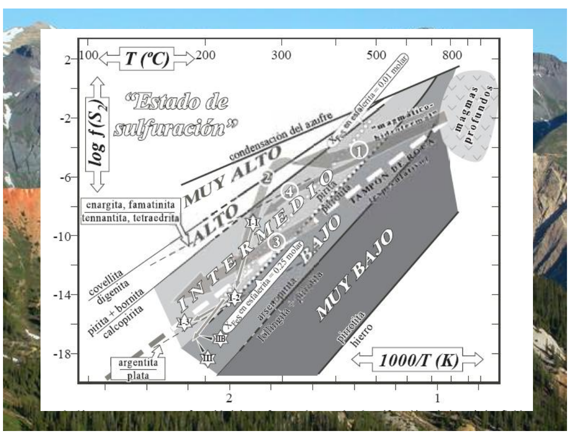

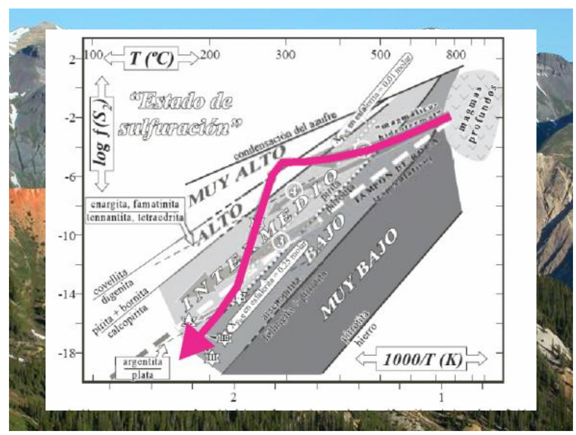

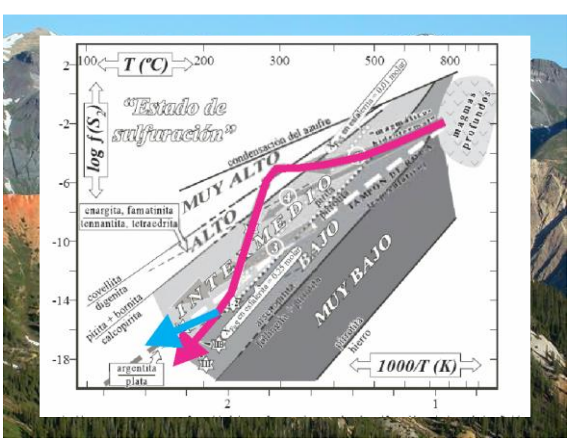

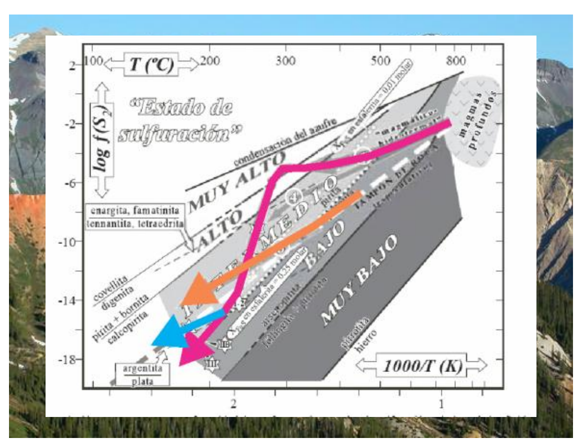

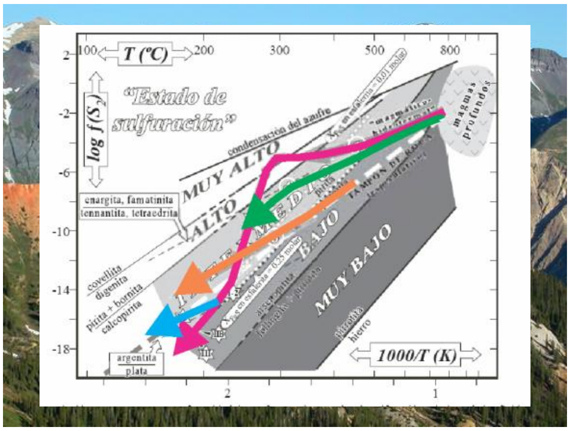

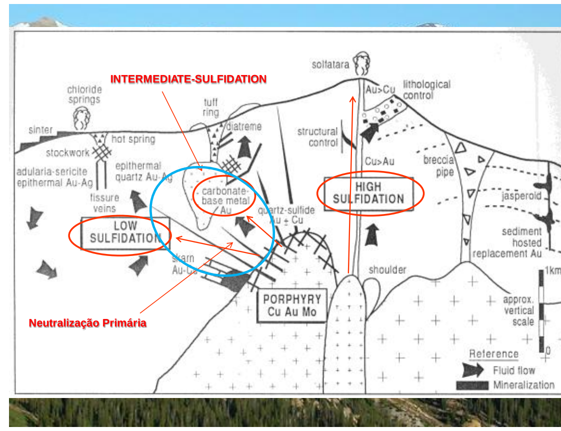

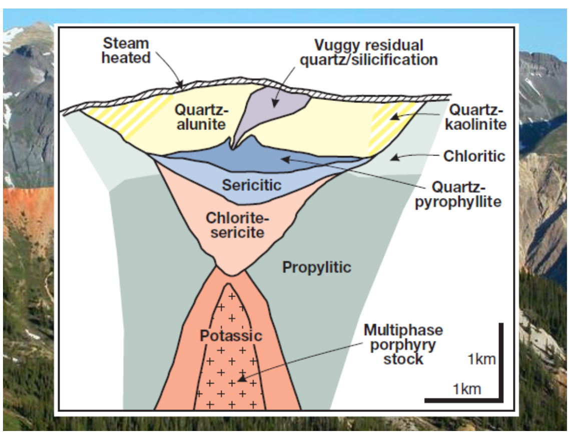

Tipo	High-sulfidation	Intermediate-Sulfidation	Low-sulfidation
Rochas vulcânicas com relações genéticas	Principalmente andesito e riodacito	Principalmente andesito e riodacito. Localmente riolito	Basalto a riolito
Ocorrência	Domos, diatremas, pórfiros	Domos, diatremas	Domos, diatremas
Minerais de alteração	Quartzo, alunita, APS, pirofilita, dickita	Sericita Adulária ausente	Adulária, esmectita, illita/sericita, roscoelita.
Forma do depósito.	Brechas, veios, disseminado	Veio, brechas, disseminado	Veios, *stockworks*, disseminado
Texturas do minério	Substituição, sulfetos maciços, veios e brechas, quartzo *vuggy*.	Brechas, veio em pente (*comb*), bandas grossas	Brechas, veios pentes (*comb*), drusas, bandas grossas e lâminas.
Ganga silicosa	Silificação maciça grossa a fina e quartzo *vuggy* residual.	Preenchimento crustiforme e em pente (*comb*) de veios de quartzo	Preenchimento crustiforme de veios quartzo, calcedônia coloforme e substituição de carbonatos
Ganga carbonática	Ausente	Comumente Inclui variedades manganesíferas	Presente, mas não manganesífera
Outras gangas	Barita em estágios tardios	Barita e silicatos manganesíferos locais	Fluorita
Abundância de sulfetos	10 a 90% vol.	5 a > 20% vol.	Tipicamente <1 a 2% vol., mas < 20% vol. quando a rocha hospedeira é basalto.
Sulfetos e Sulfosais	Enargita, luzonita, acantita, estibinita, covellita, calcopirita, tetrahedrita, esfalerita	Esfalerita, galena, tetrahedrita, calcopirita	Pirita, pirrotita, arsenopirita, esfalerita enriquecida em ferro
Metais principais	Au–Ag, Cu, As–Sb, Bi, Te, Cu–Au	Ag–Au, Zn, Pb, Cu, Mo, As, Sb	Au ± Ag
Metais secundários	Zn, Pb, Bi, W, Mo, Sn, Hg	Mo, As, Sb	Zn, Pb, Cu, Mo, As, Sb, Hg
Características notáveis	Quartzo *vuggy* Sobreposição em sistemas pórfiro.	Alguns depósitos são veios contíguos à mineralizações *high-sulfidation*	*Sinter*, calcedônia

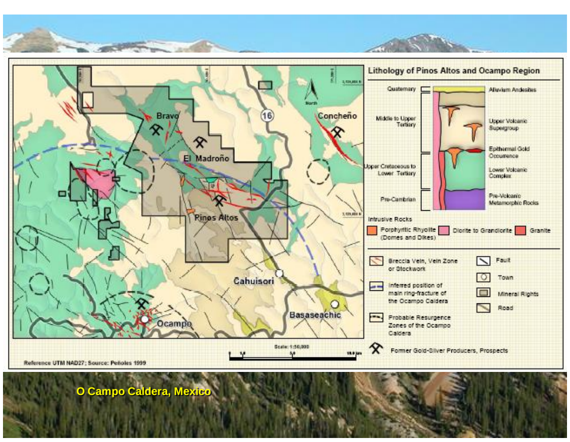

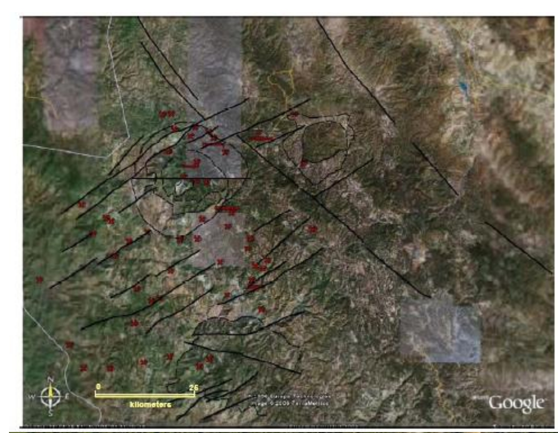

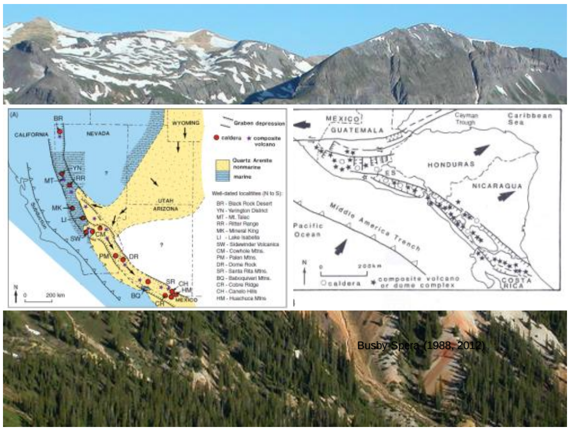

Modelo tectônico para o arco do Arizona e Nevada (Triássico Superior a Jurássico Médio)

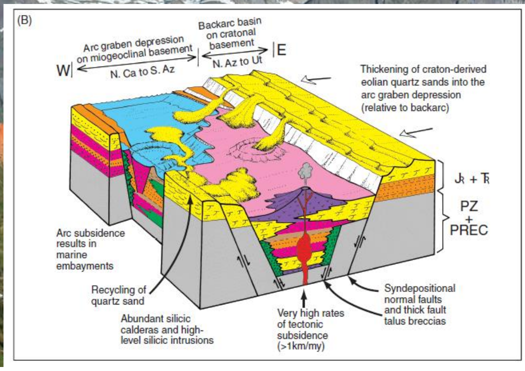

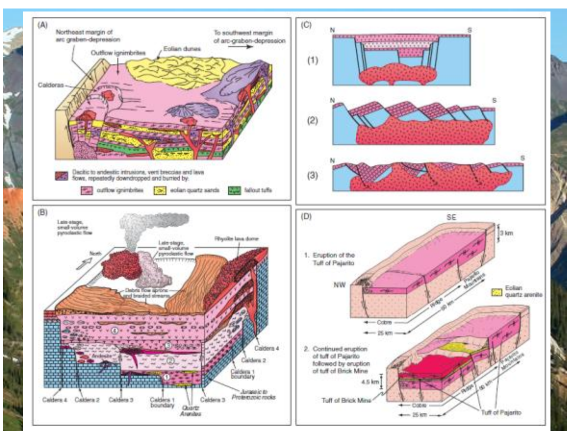

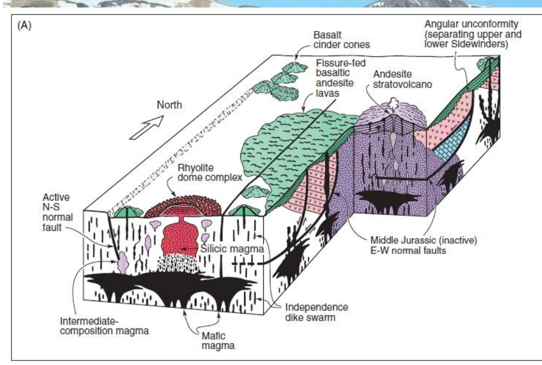

Caldeiras vulcânicas

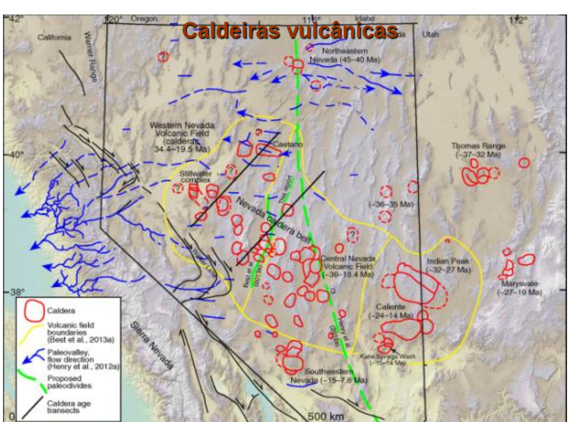

Caldeiras vulcânicas

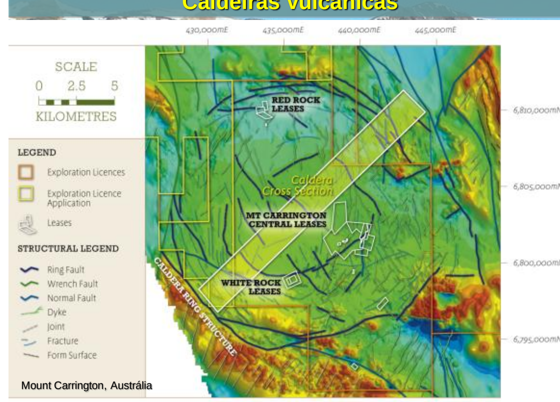

Mount Carrington, Austrália

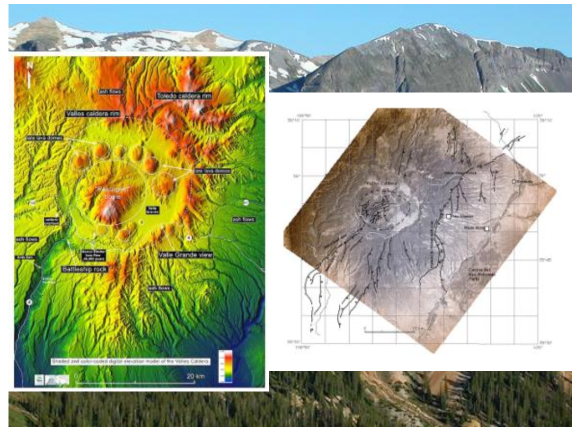
ash flows
Toledo caldera rim
Valles caldera rim
Valle Grande view
Battleship rock
ash flows
20 km


Aniakchak Caldera, Aleutian Range of Alaska (USA)
3,700-year-old volcanic *caldera* approximately 10 kilometers (6 mi)

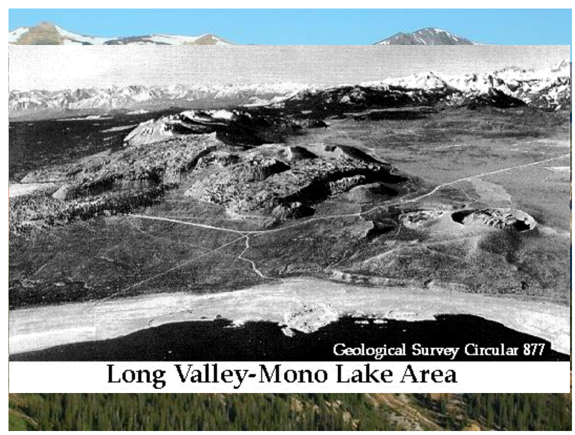
Geological Survey Circular 877
Long Valley-Mono Lake Area

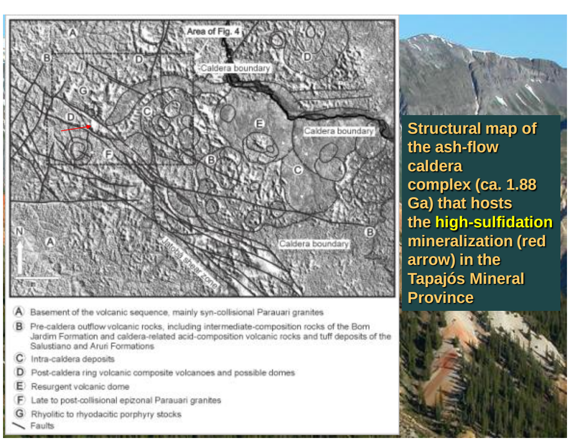
Area of Fig. 4
Caldera boundary
Caldera boundary
Caldera boundary
Jatobá shear zone
N
A Basement of the volcanic sequence, mainly syn-collisional Parauari granites
B Pre-caldera outflow volcanic rocks, including intermediate-composition rocks of the Bom Jardim Formation and caldera-related acid-composition volcanic rocks and tuff deposits of the Salustiano and Aruri Formations
C Intra-caldera deposits
D Post-caldera ring volcanic composite volcanoes and possible domes
E Resurgent volcanic dome
F Late to post-collisional epizonal Parauari granites
G Rhyolitic to rhyodacitic porphyry stocks
Faults
Structural map of the ash-flow caldera complex (ca. 1.88 Ga) that hosts the high-sulfidation mineralization (red arrow) in the Tapajós Mineral Province

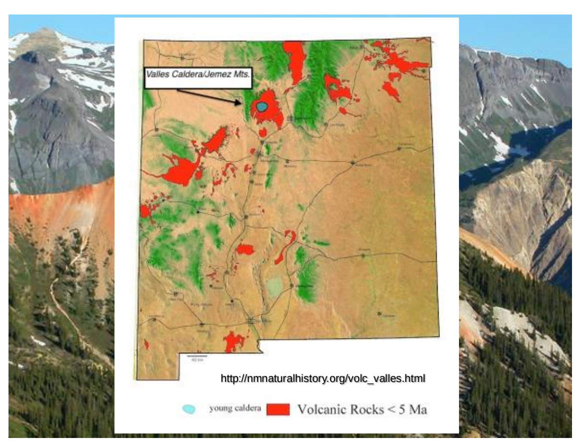
Valles Caldera/Jemez Mts.
http://nmnaturalhistory.org/volc_valles.html
young caldera
Volcanic Rocks < 5 Ma

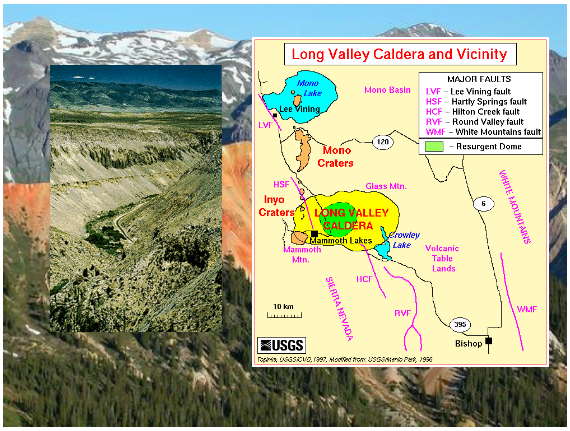

Long Valley Caldera and Vicinity
MAJOR FAULTS
LVF – Lee Vining fault
HSF – Hartly Springs fault
HCF – Hilton Creek fault
RVF – Round Valley fault
WMF – White Mountains fault
– Resurgent Dome
Mono Lake
Lee Vining
Mono Basin
Mono Craters
Inyo Craters
Glass Mtn.
LONG VALLEY CALDERA
Mammoth Lakes
Mammoth Mtn.
Crowley Lake
Volcanic Table Lands
WHITE MOUNTAINS
SIERRA NEVADA
Bishop
10 km
USGS
Topinka, USGS/CVO,1997, Modified from: USGS/Menlo Park, 1996

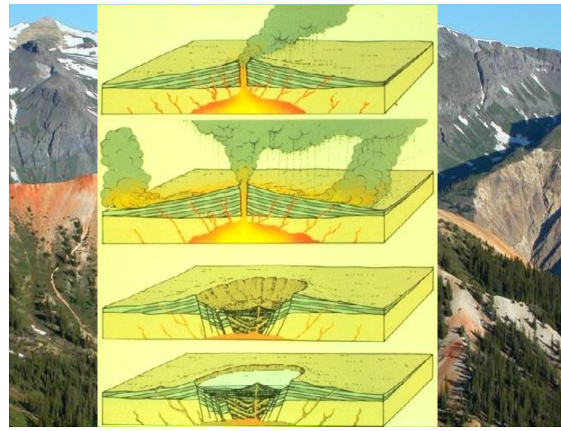

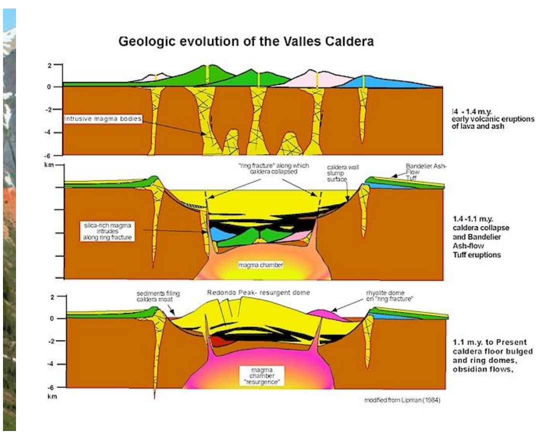

Geologic evolution of the Valles Caldera
intrusive magma bodies
14 - 1.4 m.y. early volcanic eruptions of lava and ash
"ring fracture" along which caldera collapsed
caldera wall slump surface
Bandelier Ash-Flow Tuff
silica-rich magma intrudes along ring fracture
magma chamber
1.4-1.1 m.y. caldera collapse and Bandelier Ash-flow Tuff eruptions
sediments filling caldera moat
Redondo Peak- resurgent dome
rhyolite dome on "ring fracture"
magma chamber "resurgence"
1.1 m.y. to Present caldera floor bulged and ring domes, obsidian flows,
modified from Lipman (1984)

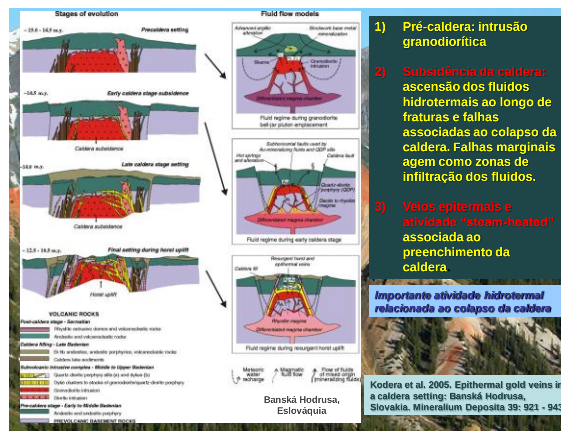

Stages of evolution
Fluid flow models
Precaldera setting
Early caldera stage subsidence
Late caldera stage setting
Final setting during horst uplift
VOLCANIC ROCKS
Banská Hodrusa, Eslováquia
1) Pré-caldera: intrusão granodiorítica
2) Subsidência da caldera: ascensão dos fluidos hidrotermais ao longo de fraturas e falhas associadas ao colapso da caldera. Falhas marginais agem como zonas de infiltração dos fluidos.
3) Veios epitermais e atividade "steam-heated" associada ao preenchimento da caldera
Importante atividade hidrotermal relacionada ao colapso da caldera
Kodera et al. 2005. Epithermal gold veins in a caldera setting: Banská Hodrusa, Slovakia. Mineralium Deposita 39: 921 - 943

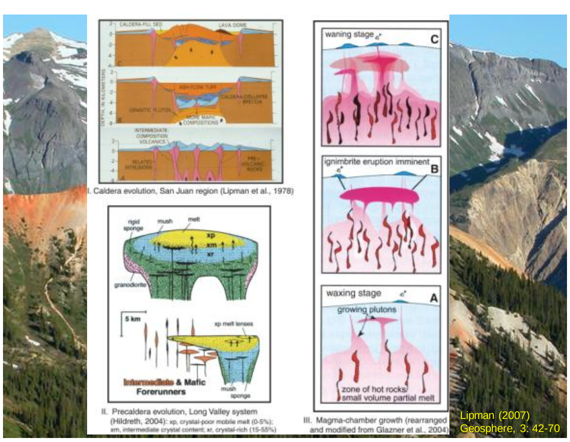

I. Caldera evolution, San Juan region (Lipman et al., 1978)
Intermediate & Mafic Forerunners
II. Precaldera evolution, Long Valley system (Hildreth, 2004)
waning stage
ignimbrite eruption imminent
waxing stage
growing plutons
zone of hot rocks small volume partial melt
III. Magma-chamber growth (rearranged and modified from Glazner et al., 2004)
Lipman (2007) Geosphere, 3: 42-70

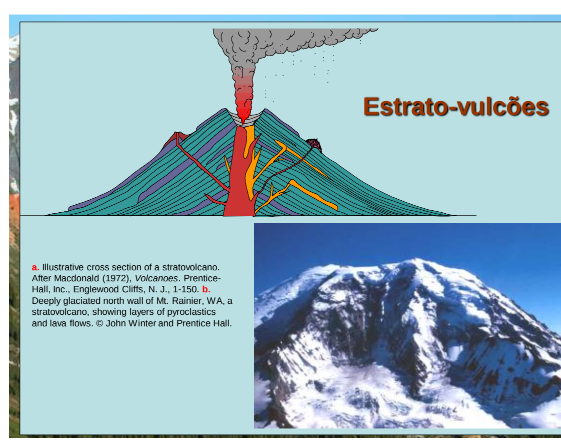

Estrato-vulcões
a. Illustrative cross section of a stratovolcano. After Macdonald (1972), Volcanoes. Prentice-Hall, Inc., Englewood Cliffs, N. J., 1-150. b. Deeply glaciated north wall of Mt. Rainier, WA, a stratovolcano, showing layers of pyroclastics and lava flows. © John Winter and Prentice Hall.

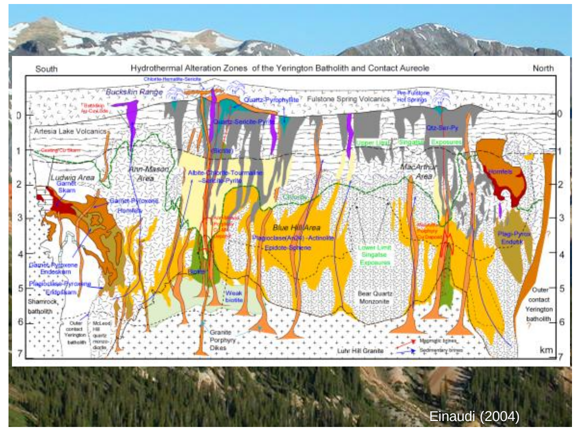

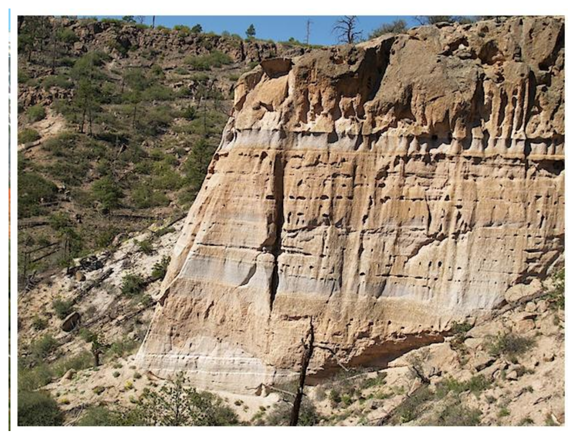

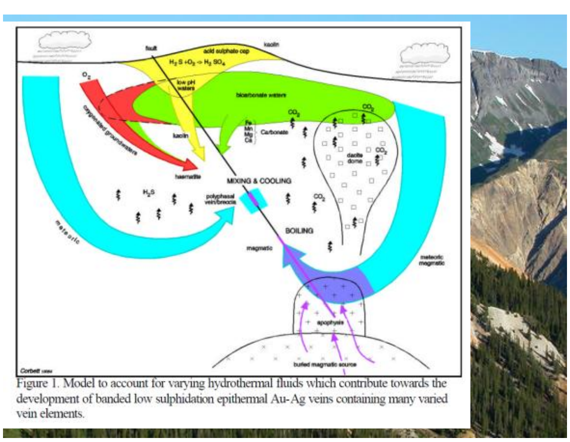

Figure 1. Model to account for varying hydrothermal fluids which contribute towards the development of banded low sulphidation epithermal Au-Ag veins containing many varied vein elements.

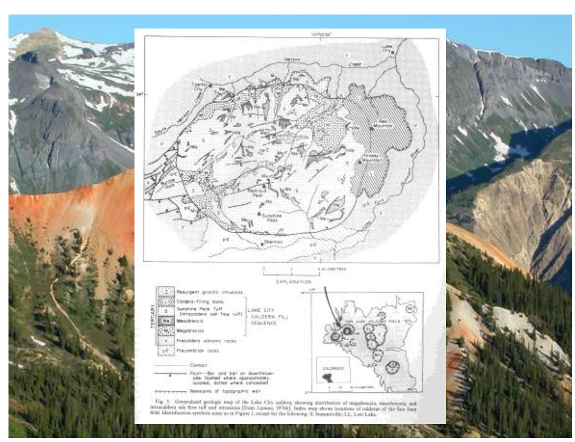

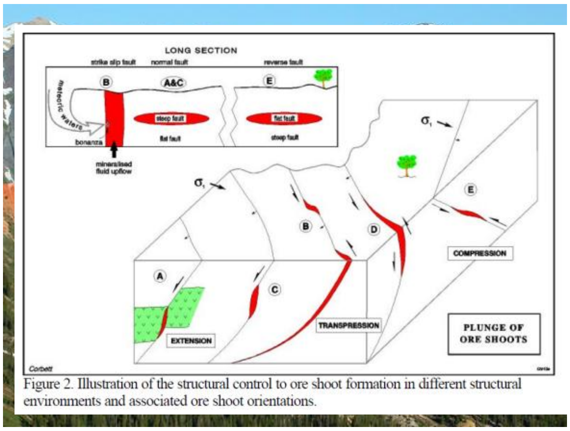
LONG SECTION
strike slip fault
normal fault
reverse fault
meteoric waters
bonanza
mineralised fluid upflow
steep fault
flat fault
PLUNGE OF ORE SHOOTS
EXTENSION
TRANSPRESSION
COMPRESSION
Corbett
Figure 2. Illustration of the structural control to ore shoot formation in different structural environments and associated ore shoot orientations.

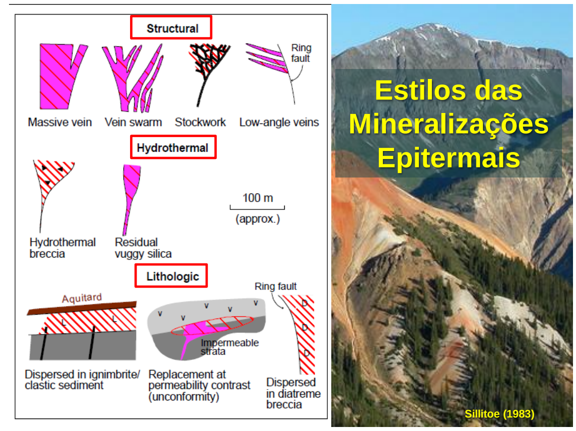
Estilos das Mineralizações Epitermais
Structural
Massive vein
Vein swarm
Stockwork
Low-angle veins
Ring fault
Hydrothermal
Hydrothermal breccia
Residual vuggy silica
100 m
(approx.)
Lithologic
Aquitard
Ring fault
Impermeable strata
Dispersed in ignimbrite/ clastic sediment
Replacement at permeability contrast (unconformity)
Dispersed in diatreme breccia
Sillitoe (1983)

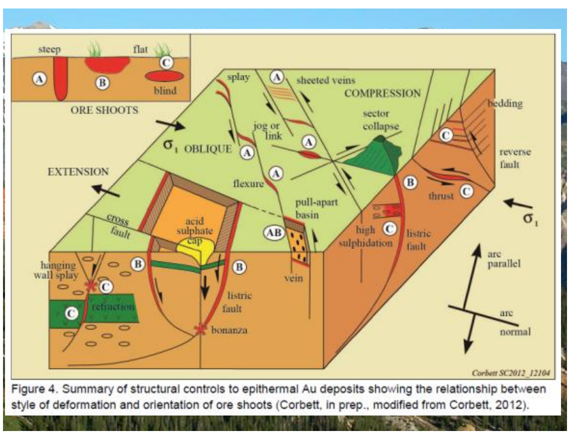
steep
flat
blind
ORE SHOOTS
EXTENSION
σ1 OBLIQUE
splay
sheeted veins
COMPRESSION
jog or link
sector collapse
bedding
reverse fault
flexure
pull-apart basin
thrust
acid sulphate cap
cross fault
high sulphidation
listric fault
hanging wall splay
refraction
vein
listric fault
bonanza
arc parallel
arc normal
Corbett SC2012_12104
Figure 4. Summary of structural controls to epithermal Au deposits showing the relationship between style of deformation and orientation of ore shoots (Corbett, in prep., modified from Corbett, 2012).

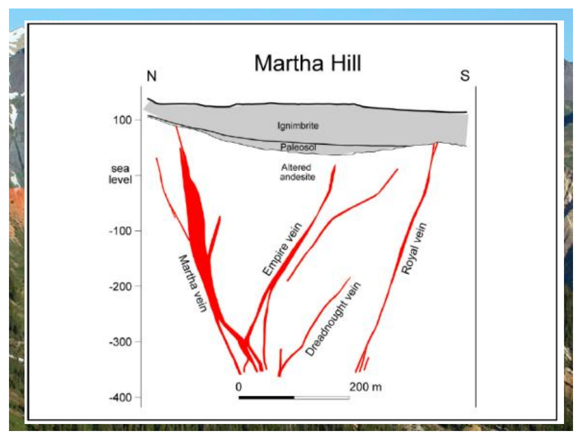
Martha Hill
N
S
100
sea level
-100
-200
-300
-400
Ignimbrite
Paleosol
Altered andesite
Martha vein
Empire vein
Dreadnought vein
Royal vein
0
200 m

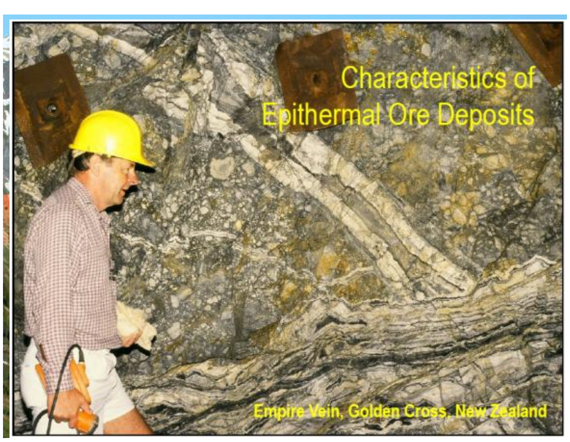
Characteristics of Epithermal Ore Deposits
Empire Vein, Golden Cross, New Zealand

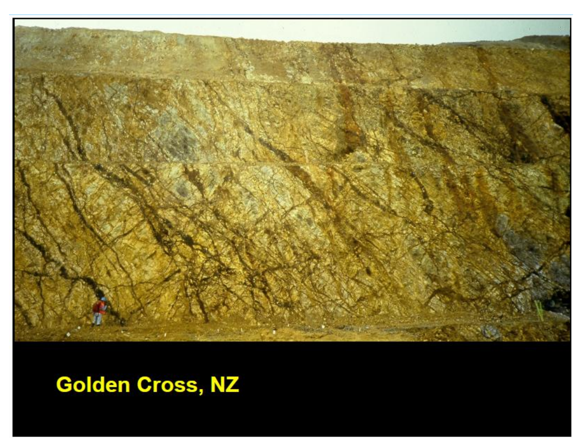
Golden Cross, NZ

Sub-tipos

1) De ebulição profunda (> 1000 m e > 300 ^{o}C)

2) De superfície (*hot springs*) (300 - 400 m)

3) Profundos, sem ebulição

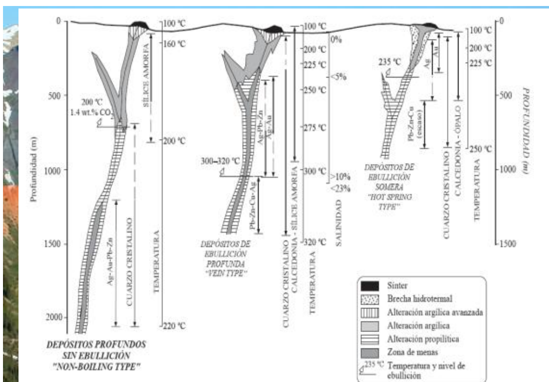

Tipos de depósitos epitermales alcalinos/neutros (baja e intermedia sulfuración) presentes en México, según su profundidad de formación relacionado al inicio del proceso de ebullición de fl uidos sódico-clorurados ascendentes (simplifi cado de Albinson et al., 2001).

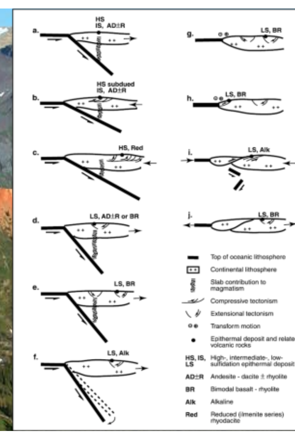

Ambiente tectônico das mineralizações epitermais

Mineralização *High-sulfidation*

Associa-se a rochas formadas por magmas oxidados (tipicamente cálcio-alcalinos)

Fluidos predominantemente magmáticos, com pouca participação de águas meteóricas.

Fluidos ácidos e oxidados

Alteração argílica avançada e sulfatos (alunita)

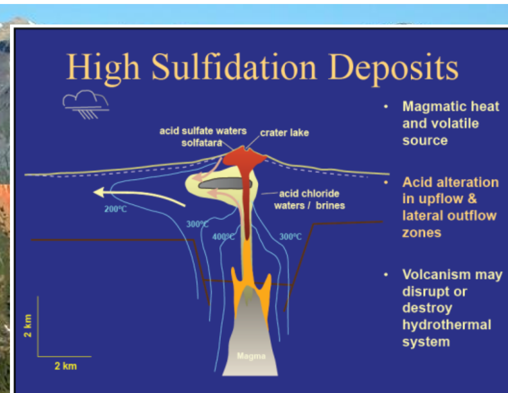

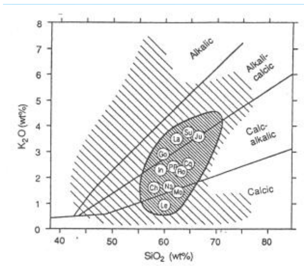

Características químicas dos magmas geneticamente associados às mineralizações *High-Sulfidation* (Arribas Jr., 1995)

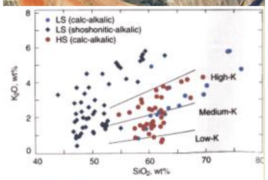

Fig. 2.4 Plot of K_2O versus SiO_2 for volcanic rocks [15] thought to be genetically related to Au mineralization [1,31,50]. HS deposits appear to be associated with a narrow range of igneous rock composition, dominated by dacite and andesite. LS deposits are largely associated with andesite and

Nos sistemas *high-sulfidation* os vapores ricos em SO_2 e HCl são absorvidos pelas águas superficiais, fazendo com que haja a desproporcionalização em H_2SO_4 e H_2S.

Esse fluido ácido (pH = 0 a 2) reage extensivamente com as rochas em profundidades baixas e as lixivia intensamente, resultando em alteração argílica avançada (caolinita, dickita, pirofilita, diásporo e alunita). Essa zona passa externamente para alterações argílicas com menor volume de argilas e com aumento proporcional da illita ou da esmectita e essa passa para zona de alteração propilítica (albita, calcita, clorita e epidoto) e clorítica.

Ametista é comum.

O fluido ácido é progressivamente neutralizado pelas reações com as rochas hospedeiras em condutos.

White & Hedenquist (1995)

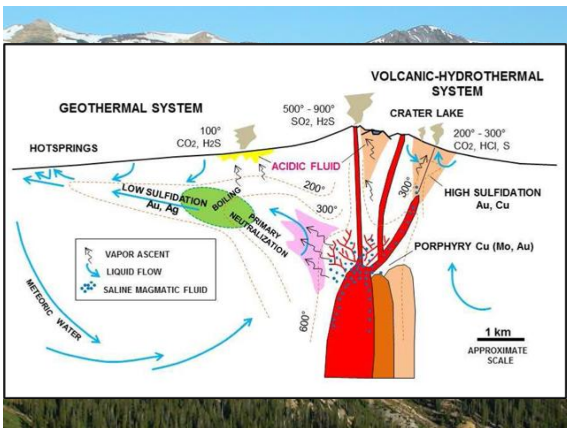

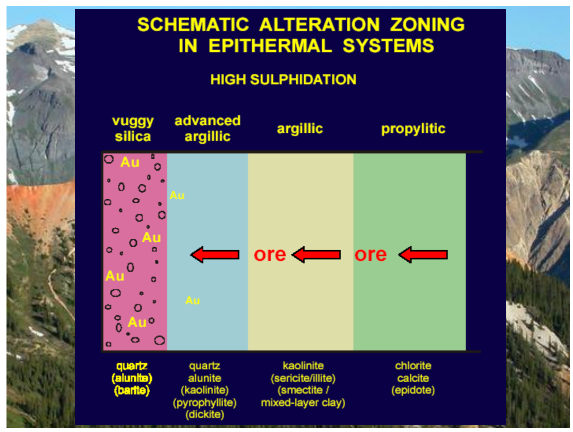

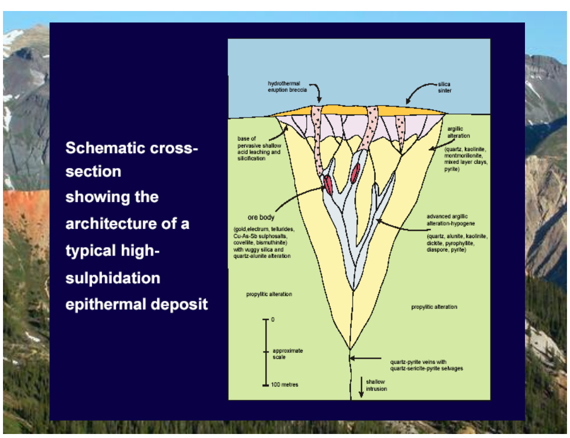

No topo do sistemas podem ser formados:

- *Silica cap*, com *vuggy silica*
- Corpos de argila
- Depósitos de *sinter* (especialmente nos sistemas *low-sulfidation*)

No núcleo do sistemas hidrotermais, principalmente nas zonas de falhas se forma veios bandados e laminados e zonas silicificadas, com sílica maciça.

A mineralização ocorre como vênulas de sulfetos no núcleo silicificado ou em sistemas de veios de quartzo microscristalino ou de calcedônia.

Calcita placóide e calcita placóide substituída por sílica.

White & Hedenquist (1995)


BOILING!!!!

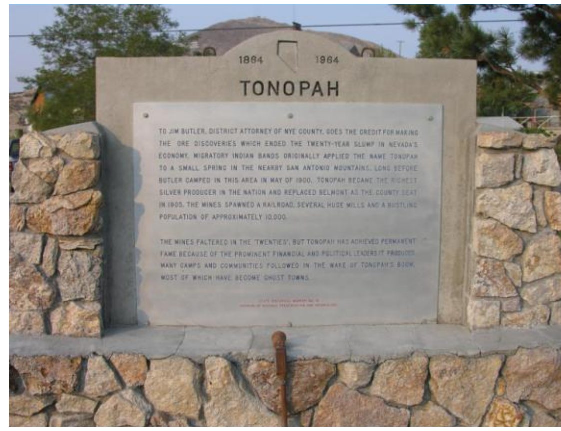
1864
1964
TONOPAH
TO JIM BUTLER, DISTRICT ATTORNEY OF NYE COUNTY, GOES THE CREDIT FOR MAKING THE ORE DISCOVERIES WHICH ENDED THE TWENTY-YEAR SLUMP IN NEVADA'S ECONOMY. MIGRATORY INDIAN BANDS ORIGINALLY APPLIED THE NAME TONOPAH TO A SMALL SPRING IN THE NEARBY SAN ANTONIO MOUNTAINS, LONG BEFORE BUTLER CAMPED IN THIS AREA IN MAY OF 1900. TONOPAH BECAME THE RICHEST SILVER PRODUCER IN THE NATION AND REPLACED BELMONT AS THE COUNTY SEAT IN 1905. THE MINES SPAWNED A RAILROAD, SEVERAL HUGE MILLS AND A BUSTLING POPULATION OF APPROXIMATELY 10,000.
THE MINES FALTERED IN THE 'TWENTIES', BUT TONOPAH HAS ACHIEVED PERMANENT FAME BECAUSE OF THE PROMINENT FINANCIAL AND POLITICAL LEADERS IT PRODUCED. MANY CAMPS AND COMMUNITIES FOLLOWED IN THE WAKE OF TONOPAH'S BOOM, MOST OF WHICH HAVE BECOME GHOST TOWNS.


FIRE DEPT
TONOPAH
HOME OF THE
STEALTH


GOLDFIELS (NEVADA)

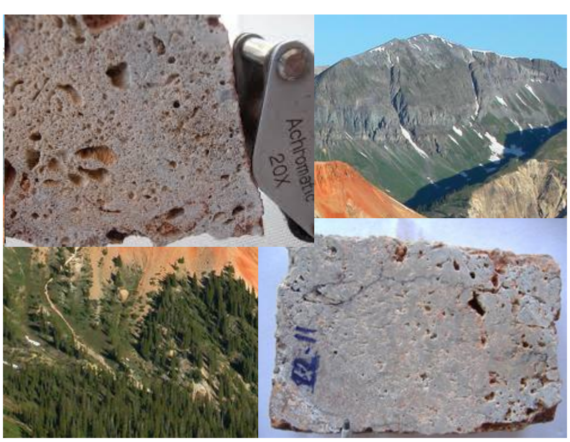
Achromatic
20X

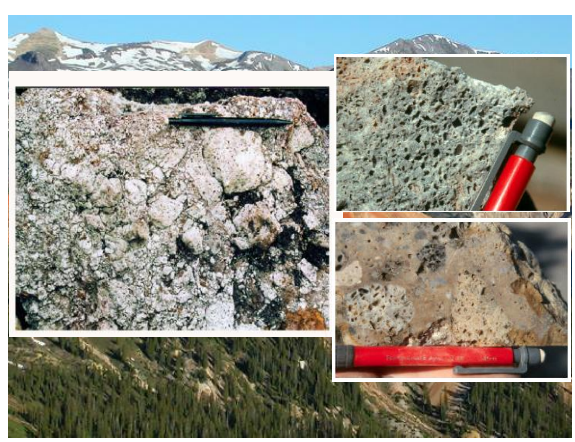

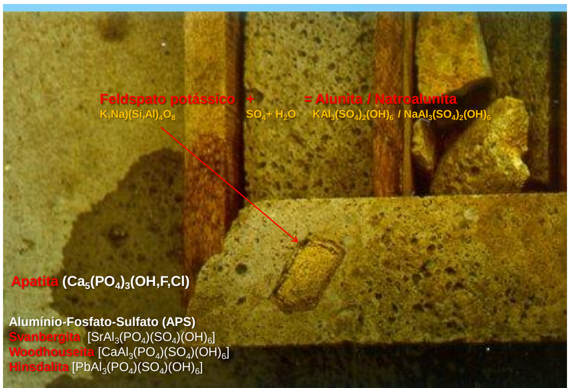

Fenocristal de feldspato potássico substituído por *alunita* em zona de sílica residual com estruturas de drusas, prospecto de Au-Ag de Marcapunta, Distrito de Colquijirca, Peru Central (Lluís Fontboté, 1998).

Alteração à sílica residual com estruturas em drusa (*vuggy quartz*) na parte central do prospecto de Au-Ag Marcapunta Au-Ag, distrito de Colquijirca, Peru Central.
(Lluís Fontboté, 1998).

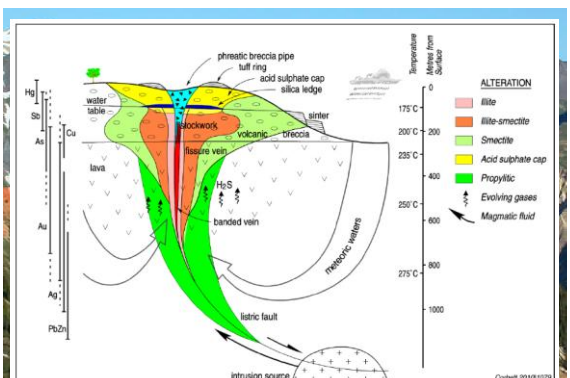

Figure 3. Model illustrating zonations in clay alteration, metals and ore type typical of banded chalcedony-ginguro epithermal Au-Ag veins (from Corbett, in prep.).

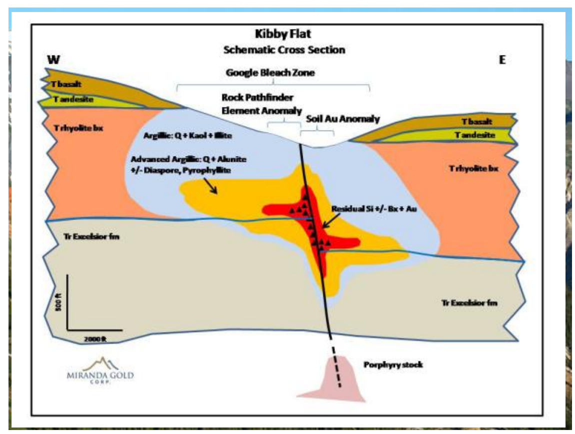

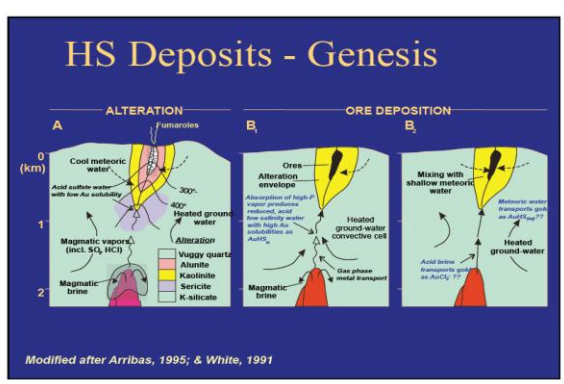

(A) Início da alteração argílica avançada dominada por vapor magmático
(B1) Absorção de vapor de altas pressões pelo arraste de células de águas meteóricas, mistura de fluidos magmático–meteóricos mineralizados
(B2) Ascensão de salmouras magmáticas enriquecidas de metais e misturadas com águas meteóricas mais frias.

Figure 2. Oblique aerial photograph, looking south-southwest, of the Summitville Mine and vicinity. The mine is located just east of the continental divide at an elevation of 3800 meters (11,500 ft). Total yearly snowfall is approximately 7–11 meters (20-35 ft). Photo by IntraSearch, Inc.

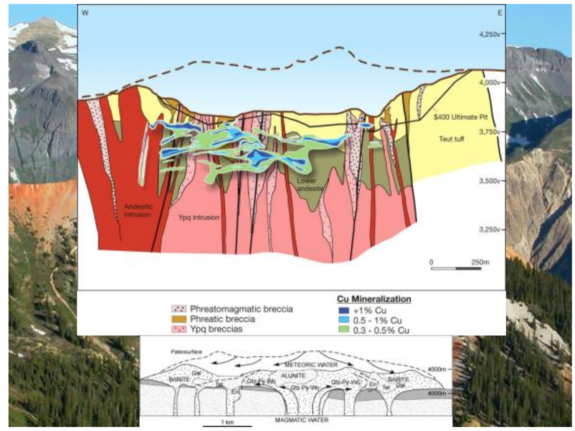

Chelopech Cu-Au Epithermal Deposit (Moritz *et al.*, 2005)

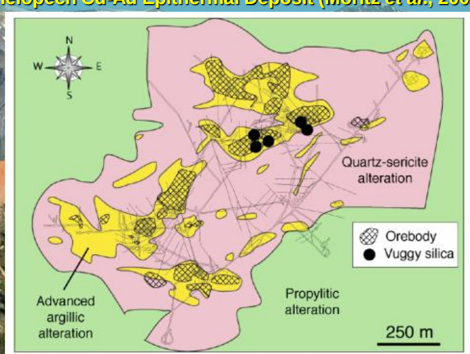

Fig. 1. Horizontal section, level 405.

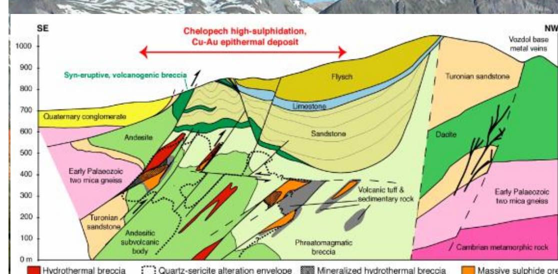

Fig. 2. Cross-section through the Chelopech deposit based on surface and underground mapping, extensive drillcore descriptions and observations, and including information from Popov and Kovachev (1996) for the north-western part at Vozdol. The present mining level is at ~400m. Rock units are Late Cretaceous, unless stated otherwise.

Remanescentes de vulcões de 1,97 Ga na Província Mineral do Tapajós

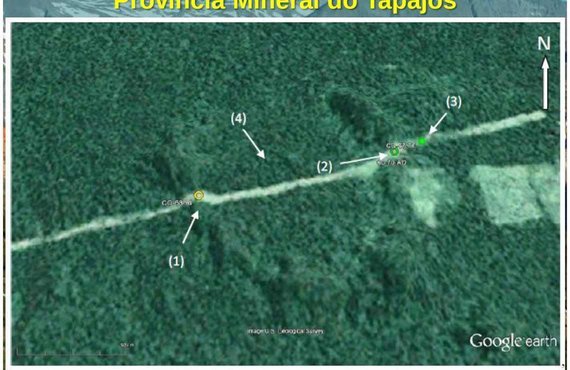

AMBIENTE "STEAM-HEATED"

Distribuição dos minerais de alteração em um ambiente "steam-heated"

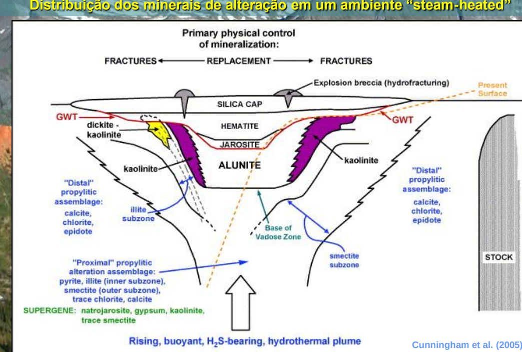

Mineralização *Low-sulfidation*

Associa-se a rochas formadas por magmas mais reduzidos,

Fluidos com grande participação de águas meteóricas (o magma pode ser apenas o motor térmico que promove a circulação de águas bacinais e meteóricas.

Podem ser formados pela neutralização primária dos fluidos hidrotermais

Fluidos reduzidos, neutros

Alteração Sericítica/Illítica com Adulária

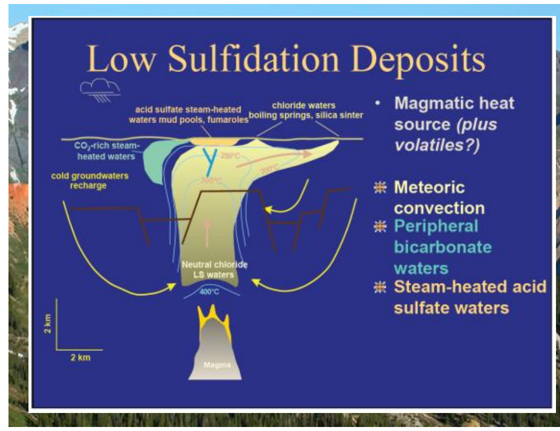

Nos sistemas *low-sulfidation*, CO_2, H_2S e NaCl são as espécies químicas principais no fluido. Grande proporção de fluido meteórico

O *boiling* é o principal processo de deposição do minério, o que causa a perda do CO_2 e do H_2S e o consequente incremento do pH.

O fluido com alto pH deposita calcita e adulária. Argilas são formadas ao redor do sistemas, com illita em profundidade (zonas mais quentes) e illita-esmectita interestratificada seguida por esmectita nas partes superiores e frias do sistema.

Associam-se zeólitas (em temperaturas baixas) e epidoto (em temperaturas altas), além de biotita e anfibólios, quando a temperatura é maior que 280 ºC.

A mineralização ocorre em cavidades em veios bandados e brechados, comumente com quartzo arroxeado (ametista)

White & Hedenquist (1995)

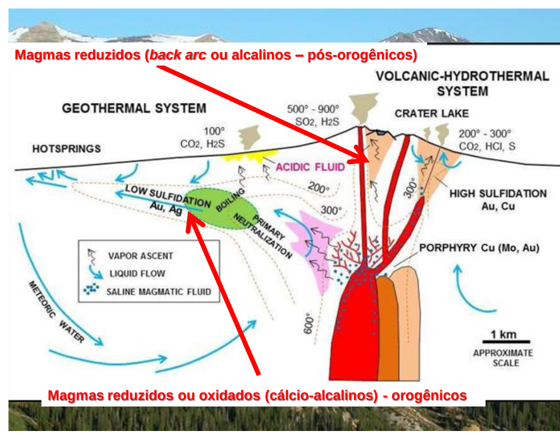

Adularia

$KAlSi_3O_8$

Monoclínico (pseudo-ortorrômbica)

Dureza: 6,0

Cor: branca, incolor, rósea, laranja vermelha, azul clara, verde clara, marrom, cinza.

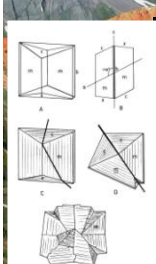

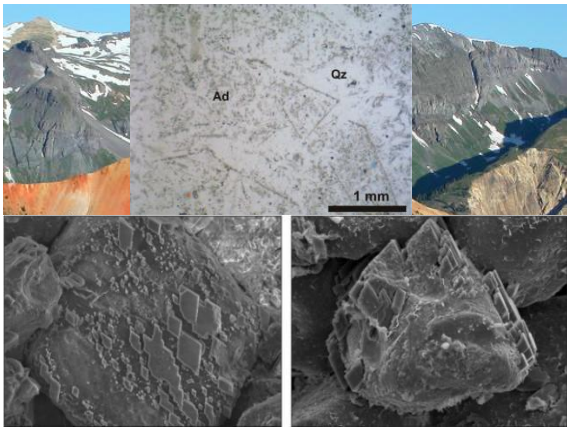

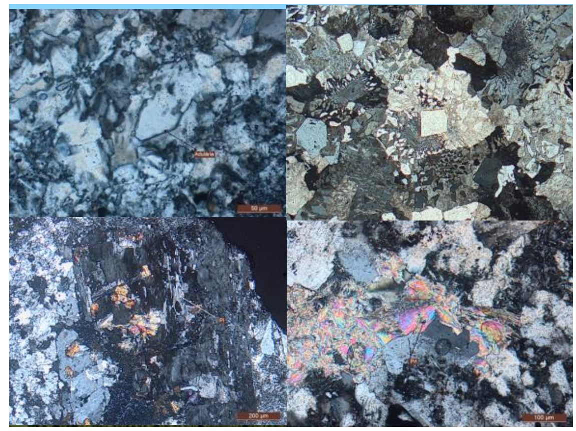

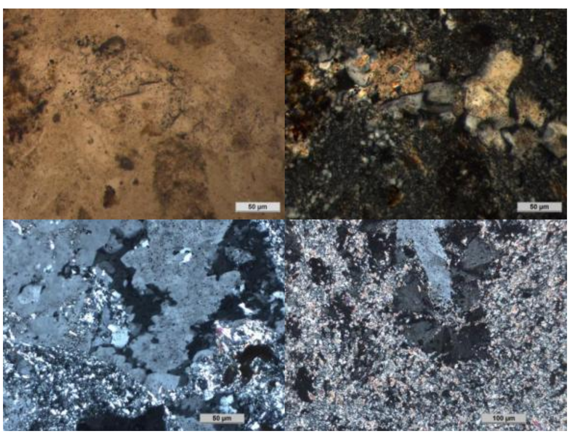

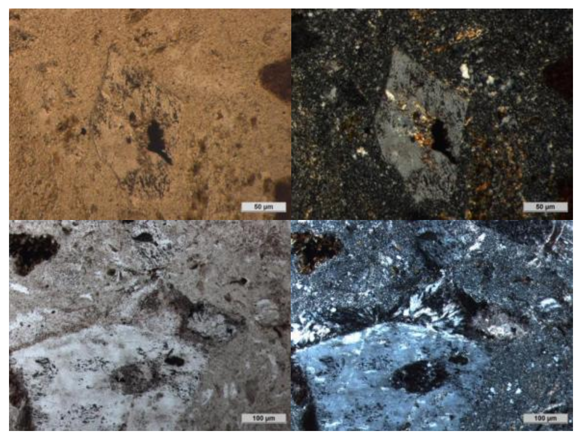

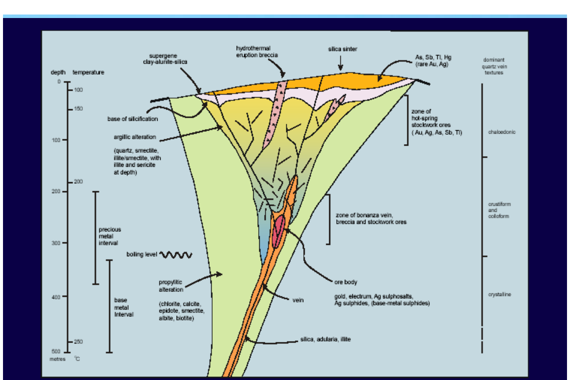

Schematic cross-section showing the architecture of a typical low-sulphidation deposit

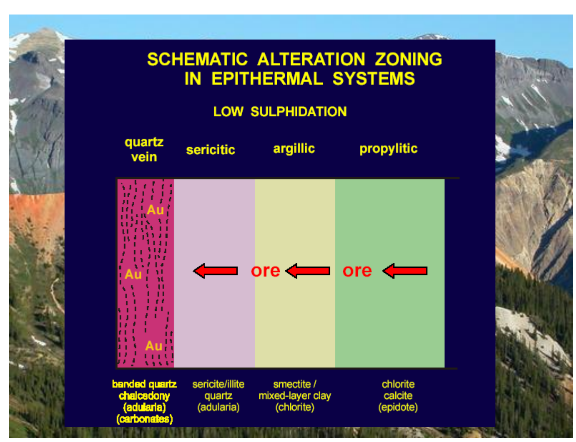

CARACTERÍSTICAS DOS DEPÓSITOS DE OURO EPITERMAIS *LOW-SULFIDATION*

1) Arcos vulcano-plutônicos em margens continentais e de ilhas oceânicas, e em zonas de *back arcs*

2) Associam-se a sistemas de falhas regionais em níveis crustais rasos, grabens, caldeiras, estratovulcões, complexos de domos e diatremas

3) Hospedados em andesitos, riodacitos e riolitos

4) Depósitos em veios e *stockworks*, teores variando de <1 to >100 g/t e ouro muito fino (não garimpável)

5) Depósitos controlados por falhas, zonas de falhas, litotipos permeáveis e brechas de falhas e hidrotermais

6) Alteração variando de silicificação (proximal), sericítica com adulária, argílica e propilítica (distal)

7) Quartzo com texturas *open-fill*, crustiforme, coloforme bandada, *comb*, *cockade* e *bladed*

8) Ganga: quartzo, chalcedônia, ametista, carbonato, adulária, barita e fluorita

9) Minério com electrum, ouro, pirita prata e esfalerita, galena, tetraedrita e calcopirita subordinados

10) Conteúdos de metais: Au, Ag (Zn, Pb, Cu, Mo, As, Sb, Te, Se, Hg, Ba, F , Mn)

11) Idades principalmente terciária e quaternárias

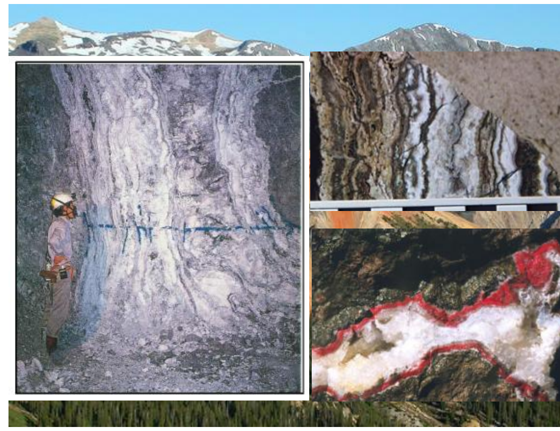

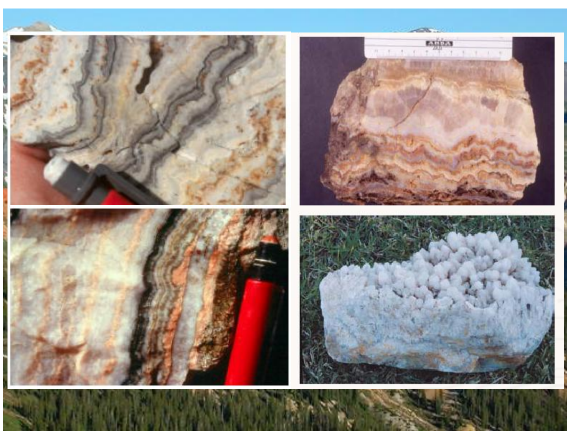

Gold-bearing quartz stockwork in low-sulphidation deposit, Ecuador

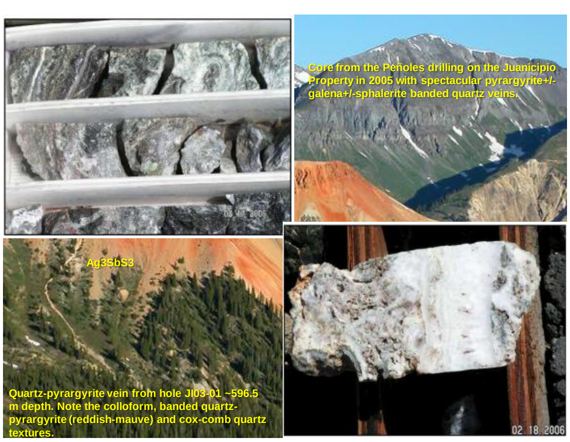

http://www.photovolcanica.com/VolcanoInfo/Wai-O-Tapu/NZ07_8800.jpg


skyewalkers.com


E
5 mm
Boudreau & Lynne (2012), JVGR, 247/248: 1-8

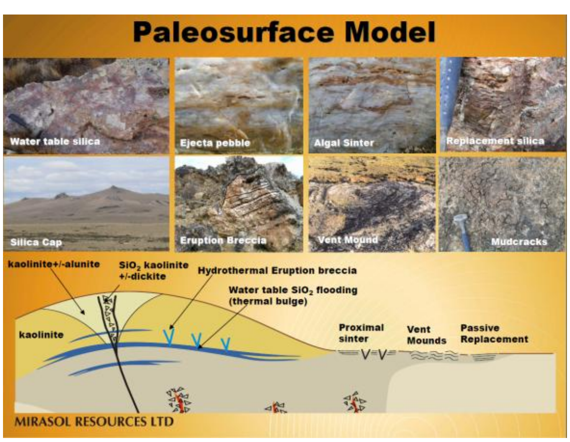
Paleosurface Model
Water table silica
Ejecta pebble
Algal Sinter
Replacement silica
Silica Cap
Eruption Breccia
Vent Mound
Mudcracks
kaolinite+/-alunite
SiO$_2$ kaolinite +/-dickite
Hydrothermal Eruption breccia
Water table SiO$_2$ flooding (thermal bulge)
kaolinite
Proximal sinter
Vent Mounds
Passive Replacement
MIRASOL RESOURCES LTD


Hydrothermal Eruption Breccia
Recrystalised Laminated Silica

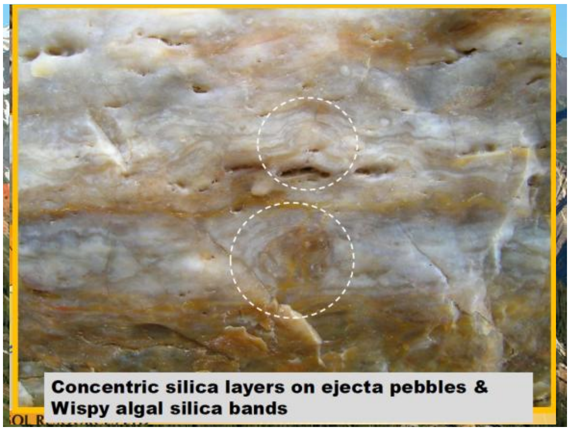
Concentric silica layers on ejecta pebbles &
Wispy algal silica bands


Shallow aqueous. Vents
mounds & stromatolites


Ag-Au chalcedony-adularia sulphide breccias


STAEDTLER stick 430 F
Ag-Au colloform
quartz ginguro


Ag crustiform polymetallic vein


Jasperiodal silica (hypogene hematite) → chalcedony pyrite.
Mixing oxidized and reduce fluids. 10's ppb Au 1 – 20 ppm Ag

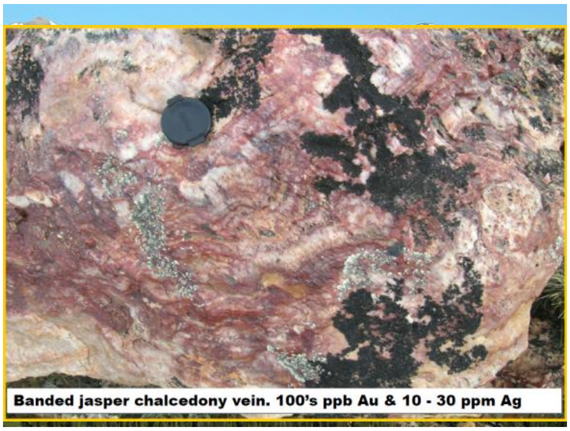
Banded jasper chalcedony vein. 100's ppb Au & 10 - 30 ppm Ag


Main Ore Zone - Felted bladed textures Colloform
Chalcedony with ginguro


Crystalline & Saccharoidal quartz + coarse bladed textures
typically poorly mineralized (may be ore grade in rare cases)

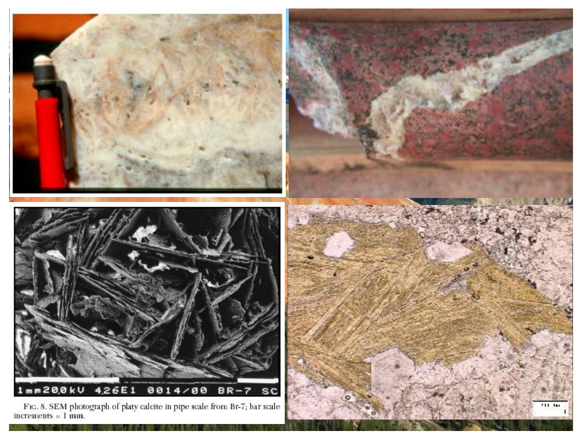
1mm20.0kV 4.26E1 0014/00 BR-7 SC
FIG. 8. SEM photograph of platy calcite in pipe scale from Br-7; bar scale increments = 1 mm.


Yilmaz et al. (2013) Turkish Journal of Earth Sciences, 22: 485-522

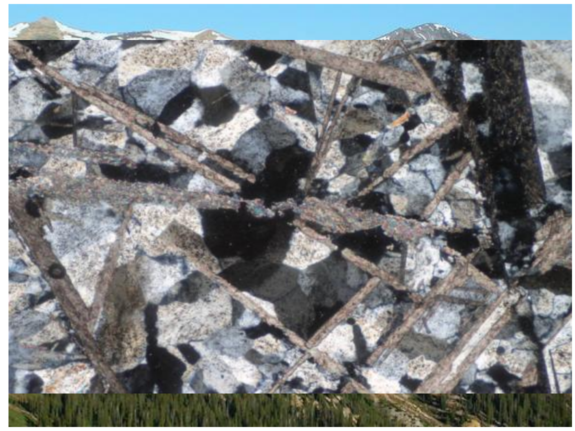

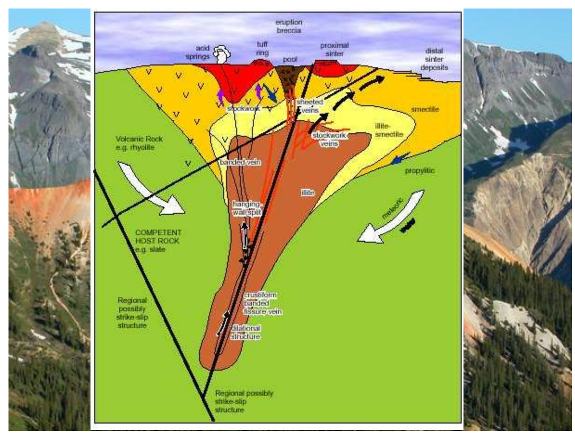

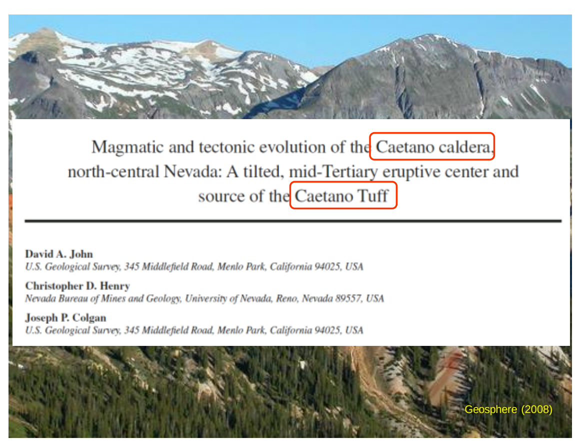
Magmatic and tectonic evolution of the Caetano caldera, north-central Nevada: A tilted, mid-Tertiary eruptive center and source of the Caetano Tuff

David A. John
U.S. Geological Survey, 345 Middlefield Road, Menlo Park, California 94025, USA

Christopher D. Henry
Nevada Bureau of Mines and Geology, University of Nevada, Reno, Nevada 89557, USA

Joseph P. Colgan
U.S. Geological Survey, 345 Middlefield Road, Menlo Park, California 94025, USA

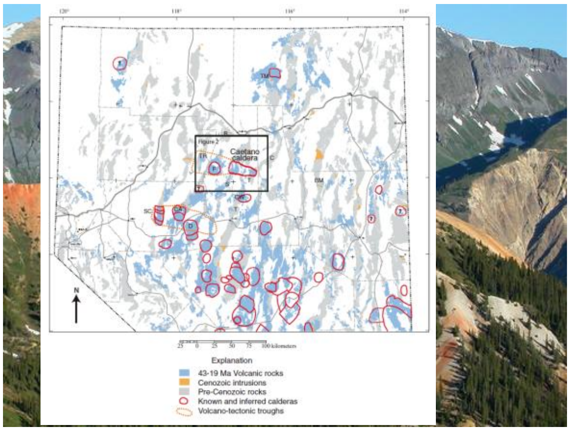

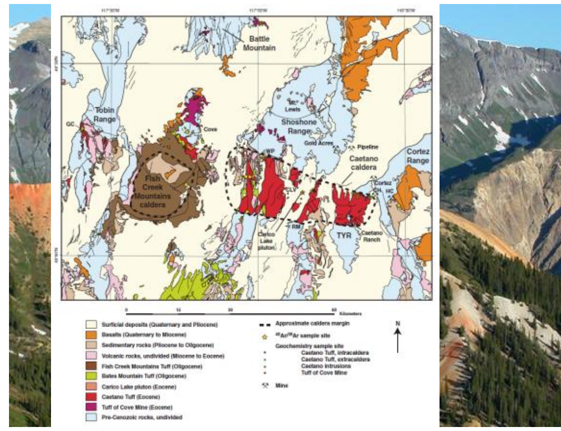

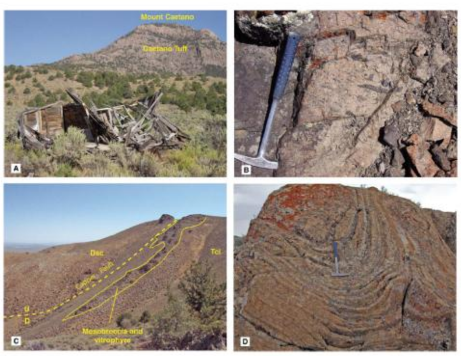

Figure 7. Photographs showing aspects of the Caetano caldera and Caetano Tuff. (A) View of Mount Caetano looking east. Mount Caetano is composed of densely welded lower unit of the Caetano Tuff that dips ~40–45° east (away) from photo. Total topographic relief is ~500 m. Remains of Caetano Ranch in foreground. (B) Strongly flattened crystal-rich pumice (fiamme) in densely welded basal vitrophyre in Caetano Tuff near Wenban Spring in northern Toiyabe Range. Hammer is 46 cm long. (C) View looking north of caldera margin in northern Toiyabe Range. Devonian Slaven Chert (Dsc) faulted against intracaldera Caetano Tuff (Tct) along the Copper Fault. Lens of mesobreccia in Caetano Tuff is enveloped by black vitrophyre thought to have formed by quenching of hot ash against cold breccia blocks shed into the caldera during eruption. (D) Flow bands in Carico Lake pluton. Hammer is 46 cm long.

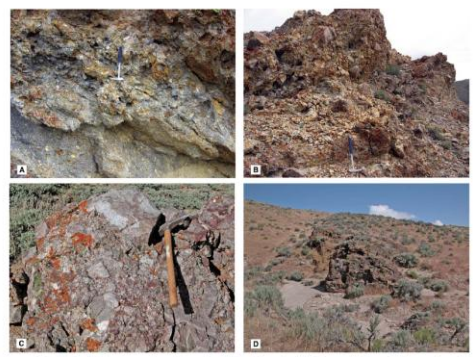

Figure 13. Photographs showing breccias in the Caetano caldera. (A) Approximately 10-m-thick mesobreccia lens in lower unit of Caetano Tuff near south margin of caldera just north of Red Mountain. Mesobreccia composed of angular fragments (up to 50 cm) of Paleozoic quartzite, argillite, and chert, Tertiary andesite, and white pumice in matrix of finely ground Paleozoic rocks. Hammer is 46 cm long. (B) Interbedded coarse, clast-supported mesobreccia and lithic-rich Caetano Tuff near south margin of caldera north of Red Mountain. Blocks are mostly Paleozoic quartzite and argillite and locally reach 2 m in diameter. Hammer is 46 cm long. (C) Brecciated Paleozoic quartzite block in mesobreccia at Wilson Pass. Hammer is 55 cm long. (D) Large block of brecciated Paleozoic chert enclosed in Caetano Tuff near base of upper unit ~0.5 km north of Tub Spring. Block is ~5 m in maximum dimension and is ~4 km from the nearest exposed caldera margin.


MANHATTAN

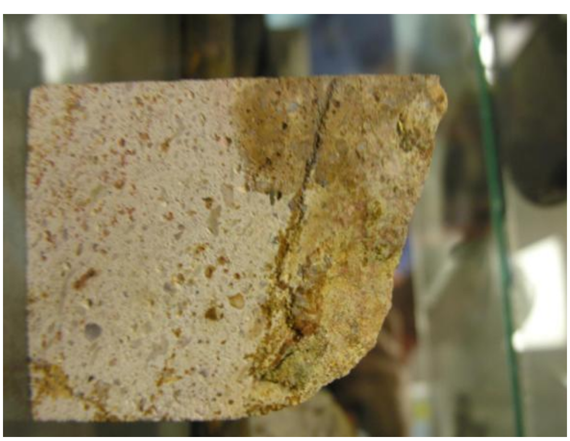


RMGC ALTERATION
MEGASCOPIC


Mineralização *Intermediate-Sulfidation*


Tipicamente enriquecida em sulfetos de metais de base (calcopirita, galena, esfalerita) e carbonatos com manganês ou de manganês (calcita manganesífera e rodocrosita)

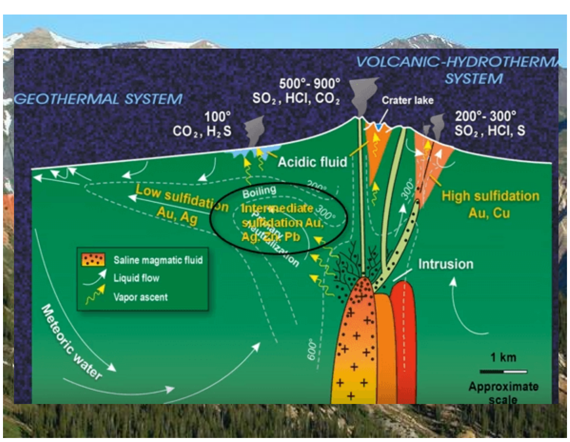
VOLCANIC-HYDROTHERMA
SYSTEM
GEOTHERMAL SYSTEM
500°- 900°
SO2, HCl, CO2
Crater lake
100°
CO2, H2S
200°- 300°
SO2, HCl, S
Acidic fluid
Low sulfidation
Au, Ag
Boiling
Intermediate sulfidation Au, Ag, Zn, Pb
High sulfidation
Au, Cu
Saline magmatic fluid
Liquid flow
Vapor ascent
Intrusion
Meteoric water
1 km
Approximate scale


► Presença local de adulária ou de pirofilita
► Presença de carbonatos – calcita e calcita manganesífera
► Ricas em sulfetos de metais de base (calcopirita, galena, esfalerita)

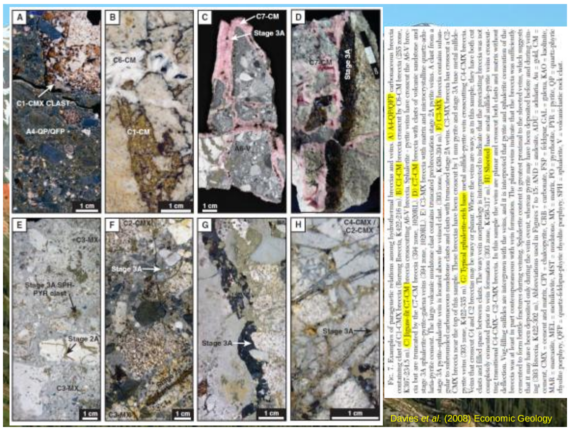

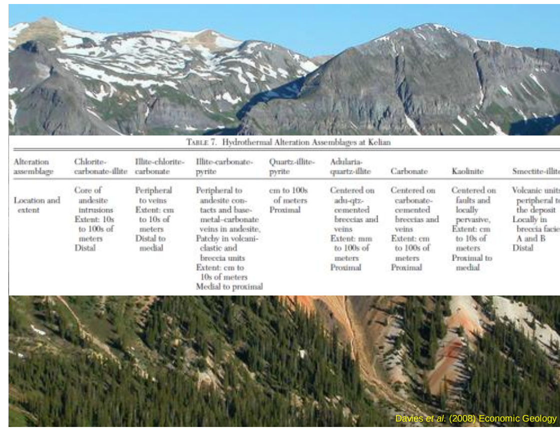

TABLE 7. Hydrothermal Alteration Assemblages at Kelian

Alteration assemblage	Chlorite-carbonate-illite	Illite-chlorite-carbonate	Illite-carbonate-pyrite	Quartz-illite-pyrite	Adularia-quartz-illite	Carbonate	Kaolinite	Smectite-illite
Location and extent	Core of andesite intrusions Extent: 10s to 100s of meters Distal	Peripheral to veins Extent: cm to 10s of meters Distal to medial	Peripheral to andesite contacts and base-metal-carbonate veins in andesite, Patchy in volcaniclastic and breccia units Extent: cm to 10s of meters Medial to proximal	cm to 100s of meters Proximal	Centered on adu-qtz-cemented breccias and veins Extent: mm to 100s of meters Proximal	Centered on carbonate-cemented breccias and veins Extent: cm to 100s of meters Proximal	Centered on faults and locally pervasive, Extent: cm to 10s of meters Proximal to medial	Volcanic units peripheral to the deposit Locally in breccia facies A and B Distal

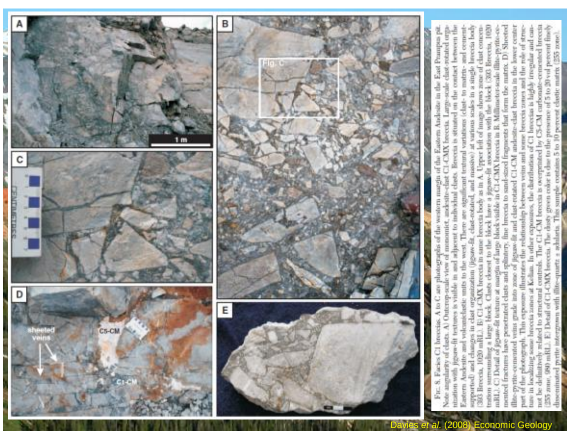

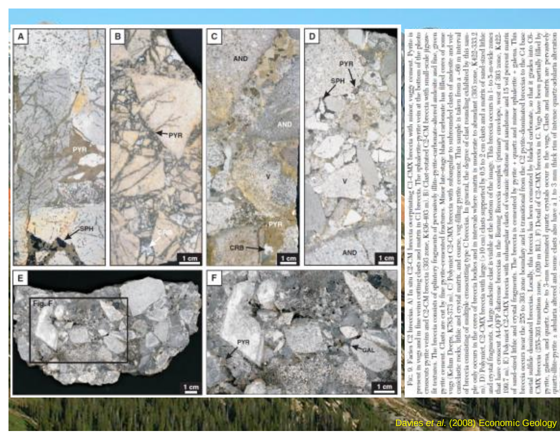

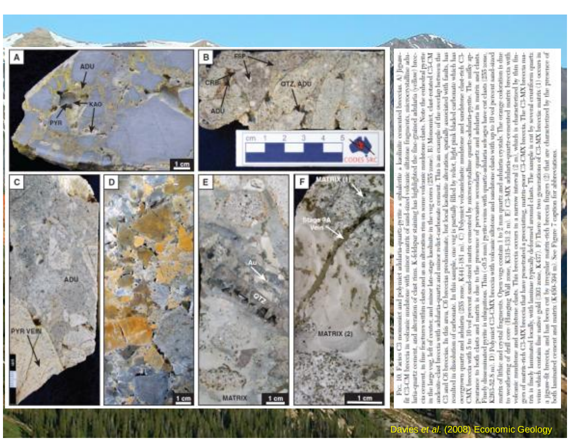

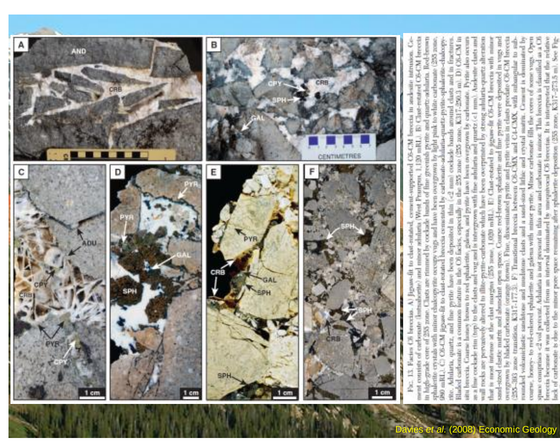

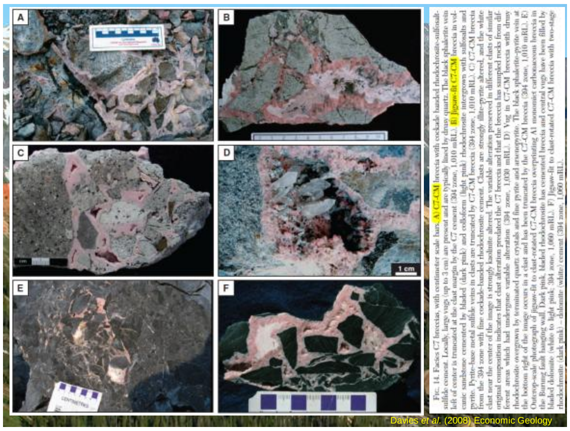
Davies et al. (2008) Economic Geology


Ore Geology Reviews 107 (2019) 434–456
Contents lists available at ScienceDirect
Ore Geology Reviews
journal homepage: www.elsevier.com/locate/oregeorev
ELSEVIER
A review of intermediate sulfidation epithermal deposits and subclassification
Le Wang, Ke-Zhang Qin, Guo-Xue Song, Guang-Ming Li
Key Laboratory of Mineral Resources, Institute of Geology and Geophysics, Chinese Academy of Sciences, Beijing 100029, PR China
Institutions of Earth Science, Chinese Academy of Sciences, Beijing 100029, PR China
University of Chinese Academy of Sciences, Beijing 100049, PR China
Department of Earth and Environmental Sciences, University of Ottawa, Ottawa K1N 6N5, Canada

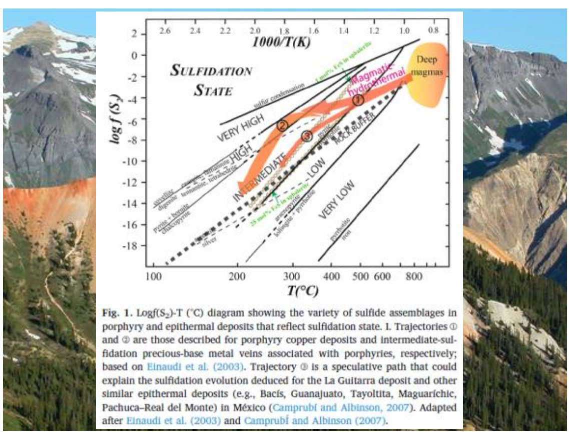
1000/T(K)
SULFIDATION STATE
log f (S2)
VERY HIGH
HIGH
INTERMEDIATE
LOW
VERY LOW
Magmatic hydrothermal
Deep magmas
T(°C)
Fig. 1. Logf(S2)-T (°C) diagram showing the variety of sulfide assemblages in porphyry and epithermal deposits that reflect sulfidation state. I. Trajectories ① and ② are those described for porphyry copper deposits and intermediate-sulfidation precious-base metal veins associated with porphyries, respectively; based on Einaudi et al. (2003). Trajectory ③ is a speculative path that could explain the sulfidation evolution deduced for the La Guitarra deposit and other similar epithermal deposits (e.g., Bacís, Guanajuato, Tayoltita, Maguarichic, Pachuca–Real del Monte) in México (Camprubí and Albinson, 2007). Adapted after Einaudi et al. (2003) and Camprubí and Albinson (2007).

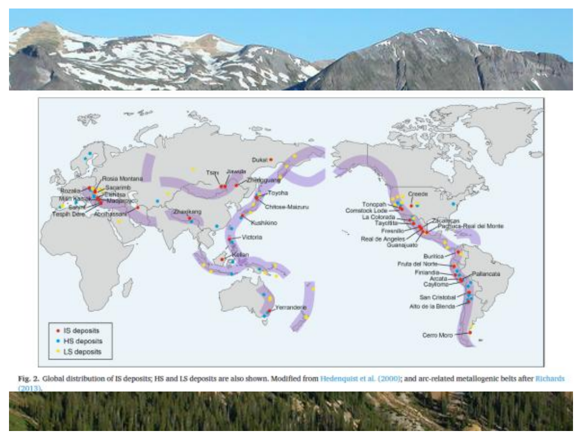
IS deposits
HS deposits
LS deposits
Fig. 2. Global distribution of IS deposits; HS and LS deposits are also shown. Modified from Hedenquist et al. (2000); and arc-related metallogenic belts after Richards (2013).

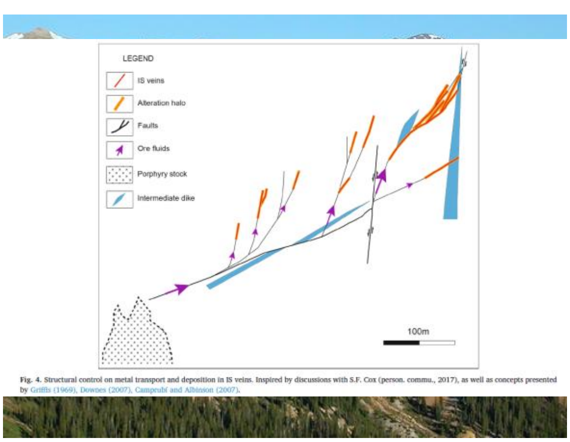
LEGEND
IS veins
Alteration halo
Faults
Ore fluids
Porphyry stock
Intermediate dike
100m
Fig. 4. Structural control on metal transport and deposition in IS veins. Inspired by discussions with S.F. Cox (person. commu., 2017), as well as concepts presented by Griffis (1969), Downes (2007), Camprubí and Albinson (2007).

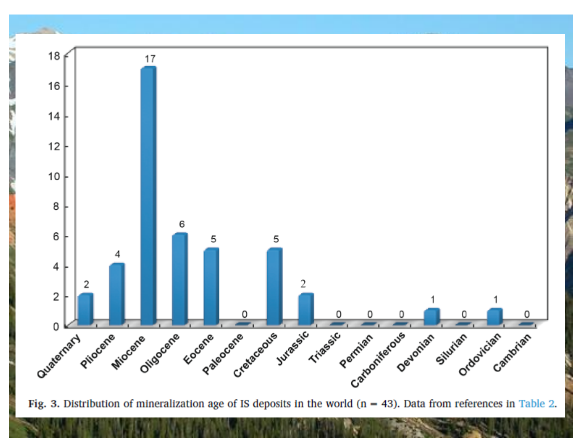
Quaternary
Pliocene
Miocene
Oligocene
Eocene
Paleocene
Cretaceous
Jurassic
Triassic
Permian
Carboniferous
Devonian
Silurian
Ordovician
Cambrian
Fig. 3. Distribution of mineralization age of IS deposits in the world (n = 43). Data from references in Table 2.

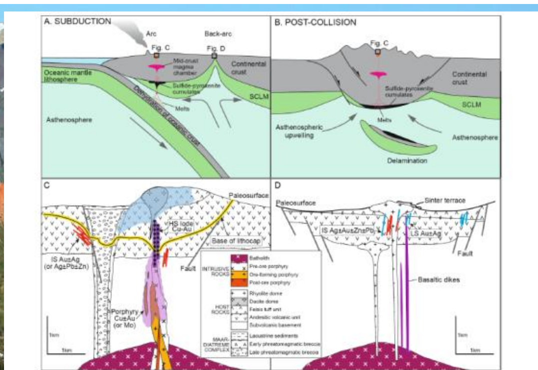

Fig. 7. Schematic diagram showing the tectonic subclassification of two IS subtypes. A. Subduction stage with a neutral-compressional stress state (modified from Richards (2011)); B. Extensional post-collision stage (modified from Richards (2011); C. Anatomy of a telescoped porphyry Cu system showing spatial interrelationships of a centrally located porphyry Cu ± Au and NC-type IS Au ± Ag system or porphyry Mo ± Cu and E-type IS Ag ± Pb ± Zn system along with possible HS deposit in a multiphase porphyry stock. Note that PMD-E-type IS are usually formed under extensional intra-arc or continental margin arc. Adapted after Sillitoe (2010); D. General model for E-type IS deposits, adapted after Sillitoe and Hedenquist (2003). SCLM = sub-continental lithospheric mantle.

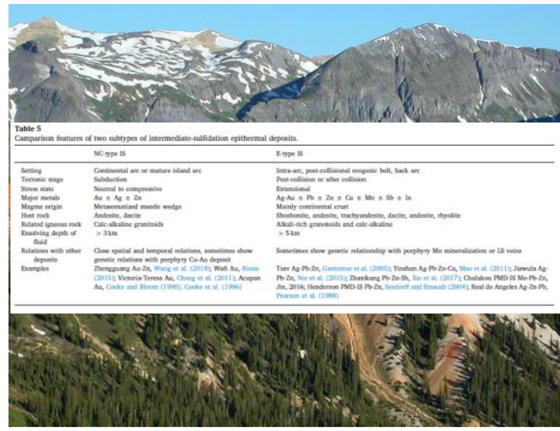

Table 5
Camparison features of two subtypes of intermediate-sulfidation epithermal deposits.

	NC-type IS	E-type IS
Setting	Continental arc or mature island arc	Intra-arc, post-collisional orogenic belt, back arc
Tectonic stage	Subduction	Post-collision or after collision
Stress state	Neutral to compressive	Extensional
Major metals	Au ± Ag ± Zn	Ag-Au ± Pb ± Zn ± Cu ± Mn ± Sb ± In
Magma origin	Metasomatized mantle wedge	Mainly continental crust
Host rock	Andesite, dacite	Shoshonite, andesite, trachyandesite, dacite, andesite, rhyolite
Related igneous rock	Calc-alkaline granitoids	Alkali-rich granotoids and calc-alkaline
Exsolving depth of fluid	> 3 km	> 5 km
Relations with other deposits	Close spatial and temporal relations, sometimes show genetic relations with porphyry Cu-Au deposit	Sometimes show genetic relationship with porphyry Mo mineralization or LS veins
Examples	Zhengguang Au-Zn, Wang et al. (2018); Wafi Au, Rinne (2015); Victoria-Teresa Au, Chang et al. (2011); Acupan Au, Cooke and Bloom (1990), Cooke et al. (1996)	Tsav Ag-Pb-Zn, Gantumur et al. (2005); Yinshan Ag-Pb-Zn-Cu, Mao et al. (2011); Jiawula Ag-Pb-Zn, Nie et al. (2015); Zhaxikang Pb-Zn-Sb, Xie et al. (2017); Chalukou PMD-IS Mo-Pb-Zn, Jin, 2016; Henderson PMD-IS Pb-Zn, Seedorff and Einaudi (2004); Real de Angeles Ag-Zn-Pb, Pearson et al. (1988)